Published by Avanti Publishers

The Global Environmental Engineers

ISSN (online): 2410-3624

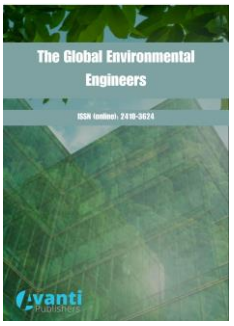

500-Year Records Demonstrating a Sharp Increase in Intensities of Three Natural Hazards at Multiple Spatiotemporal Scales in China

Zhaohua Wang[1,2], Jingxiang Yuan[1,2], Yu Peng[1,2,*], Chengru Wang[1,2] and Guoying Li[1,2]

[1]*College of Life & Environmental Sciences, Minzu University of China, Beijing 100081, China*

[2]*Key Laboratory of Ecology and Environment in Minority Areas (Minzu University of China), National Ethnic Affairs Commission, Beijing 100081, China*

ARTICLE INFO

Article Type: Research Article

Academic Editor: Hermano M. Queiroz

Keywords:
China
Disasters
500 years
Natural hazards
Spatial-temporal pattern

Timeline:
Received: November 11, 2023
Accepted: December 20, 2023
Published: December 28, 2023

Citation: Wang Z, Yuan J, Peng Y, Wang C, Li G. 500-year records demonstrating a sharp increase in intensities of three natural hazards at multiple spatiotemporal scales in China. Glob Environ Eng. 2023; 10: 18-32.

DOI: https://doi.org/10.15377/2410-3624.2023.10.3

ABSTRACT

China has experienced frequent natural disasters, including droughts, floods, and heavy snowfall. This study discusses the temporal-spatial patterns in the country since 1500. The intensity of drought in Henan and Inner Mongolia was higher than that in Guizhou and Qinghai, while little difference in flood intensity was observed among these provinces. The intensity of snow disasters in Qinghai was much higher. Except for the slightly decreasing drought trend in Henan, the three natural disasters showed a significant increase over time. Drought disasters in Guizhou, Henan, and Qinghai showed few seasonal differences, whereas those in Inner Mongolia mostly occurred in winter and spring. Floods were concentrated during the summer, while snow disasters occurred mainly during winter and spring. According to the Mann–Kendall (M–K) test, the seasonal differences in disaster trends in Guizhou, Henan, and Qinghai were unclear and similar to the overall trend. However, the disaster trends in Inner Mongolia showed seasonal differences. The spatial distribution of natural disasters in Guizhou and Henan were similar, and their changing trends were extremely scattered, while in Inner Mongolia and Qinghai, they were clustered. The spatial distribution of disaster intensity had few seasonal differences and was similar to the overall distribution. However, when considering the spatial distribution of disaster trends by season, seasonal differences were evident. This study has provided an earlier signal on how to prevent and mitigate natural disasters based on 500 years' tempo-spatial pattern, and the measures on how to improve the management practices of natural hazards under climate change were also suggested.

*Corresponding Author
Email: yuupeng@163.com
Tel: +(86) 13521015873

1. Introduction

With the acceleration of climate change, natural disasters are occurring more frequently and more severely than ever before [1-6]. Natural disasters can significantly weaken human and economic development [4, 5, 7, 8]. Owing to its complex environment, China has been acknowledged as one of the countries most vulnerable to natural disasters worldwide [6, 9], with the main types of disasters including droughts, floods, and snow. China is located in an area that frequently experiences drought [10], making it particularly vulnerable to increased drought risks due to climate change [11-13]. Droughts have harmful impacts on ecosystems and socio-economic development on a large scale [14-16] and cause significant losses [17]. For example, Liu and Diamond (2005) reported that approximately 160,000 km2 of cropland in China has been damaged by droughts, and drought-affected areas have shown an increasing trend [9, 18-20]. The 2010 spring drought caused 744 rivers to cease flowing and 564 smaller reservoirs to dry up in the Yunnan Province alone [21].

Extreme flood events are predicted to become more frequent and damaging because of the warming climate [22-25]. According to Smith *et al*. (2019) [26], the total population exposed to a 100-year flood in 18 countries (Mexico, South Africa, the Philippines, among others) was 101 million. In China, the 1998 floods of the Yangtze River caused thousands of deaths and more than USD 18 billion in direct economic losses [27]. Floods are expected to become even more severe in the future [28]. Although snow cover is an important source of water in water storage areas, heavy snow may affect the tourism industry [29], and mountain ecosystems [30], and may cause the collapse of buildings [31, 32].

If natural disasters can be predicted, prevented, or avoided, human casualties and economic losses can be greatly reduced. Therefore, it is necessary to understand the spatiotemporal patterns of natural disaster intensity. However, most previous studies have concentrated on specific types of natural disasters [6, 18, 19, 33, 34] or disasters that cause serious casualties [35]. China has a complex and diverse climate, with subtropical, warm temperate, cold temperate, and plateau climates. The climatic characteristics of an area have a significant effect on local natural disasters. Natural disasters in different climate zones also exhibit different temporal and spatial patterns. Studying these in specific climates is more targeted, which also makes the prevention of natural disasters more targeted. In this study, to understand the spatiotemporal patterns of the three main natural disasters at seasonal and annual scales over the past 500 years in the four climate zones in China, we analyzed the 500-year natural disaster intensity data for every season in different counties in the Guizhou, Henan, Inner Mongolia, and Qinghai Provinces. These results may provide support for policymakers to prevent and mitigate natural disasters.

2. Data Source

We used the official recorded drought and flood data at the county level in the study area from 1500 to 2015 from the following official records, i.e., printed books by the Inner Mongolia Government, China; Historical Materials of Natural Disasters in Past Ages in Inner Mongolia (1982) (data from B.C. 244 to A.D. 1949); Continued Edition of Historical Materials of Natural Disasters in Past Ages in Inner Mongolia (1988) (data from 1949–1986), and published books, i.e., Annals of Natural Disasters in Inner Mongolia (2001) (data from 1986–1999), and Meteorological Yearbook of China (2016) (data from 2000–2015). The intensity of droughts and flood disasters in these records was divided into three degrees, i.e., light, moderate, and severe, according to human and economic losses in the original records. A “light” intensity was simply recorded as “drought/flood occurred,” indicating a light loss; a “moderate” intensity was recorded as “large drought/flood, causing a large loss”; and a “severe” intensity indicates “great drought/flood, causing human and severe economic losses. To explore the drought–flood correlations, the light, moderate, and severe grades were quantified as 1, 2, and 3, respectively. The annual total intensity of one type of disaster in one county is the intensity multiplied by its frequency and then summed. The spatial analysis was conducted using ArcGIS 10.2. The detailed description and data sources can be referenced by Peng *et al.* 2018, and Peng *et al.* 2017 [36, 37].

3. Methods

3.1. Changing Trend Analysis

The Mann–Kendall (M–K) test is an effective tool for identifying whether trends exist in time-series data and has been widely used in natural disaster analysis. In this study, we used the Mann-Kendall (M-K) test to analyze the changing trend of natural disasters at 1-quarter and 1-, 5-, 10-, and 50-year intervals, respectively.

For a time series, the M-K test statistics can be defined as follows:

$$S = \sum_{i=1}^{n-1} \sum_{j=i+1}^{n} \operatorname{sgn}(x_j - x_i), \tag{1}$$

where

$$\operatorname{Sgn}(x_j - x_i) \begin{cases} 1 & x_j - x_i > 0 \\ 0 & x_j - x_i = 0 \\ -1 & x_j - x_i < 0 \end{cases}. \tag{2}$$

Here, xi and xj are the disaster areas at times i and j, respectively, and n is the number of samples. The value of S will be positive if there is an increasing trend and negative if there is a declining trend. The significance of the trend can be calculated by comparing the standardized variable Z in Eq. (3) with the standard normal variable at the expected significance level P. Var indicates the variance of S.

$$Z = \begin{cases} \dfrac{S-1}{\sqrt{\operatorname{Var}(S)}} & S > 0 \\ 0 & S = 0 \\ \dfrac{S}{\sqrt{\operatorname{Var}(S)}} & S < 0 \end{cases} \tag{3}$$

3.2. Spatial Pattern Change

However, the spatial distribution of disasters is not even. Thus, it is necessary to quantify changes to spatial patterns of disasters. In our study, Moran's I was employed to evaluate the spatial patterns of disasters. Moran's I is commonly used to measure the degree of spatial concentration or dispersion of disasters at a global scale, the index of which ranges from –1 to 1, indicating a clustered to dispersed pattern.

$$I = \frac{n}{s} \frac{\sum_{i=1}^{n} \sum_{j=1}^{n} \omega_{ij} (x_i - \bar{x})(x_j - \bar{x})}{\sum_{i=1}^{n} (x_i - \bar{x})^2}, \tag{4}$$

where n is the number of observations, s is the aggregate of all spatial weights, x_i, and x_j are the observations for areas i and j, $\bar{x}$ is the mean of the observations, it is the spatial weight between area i and j, and negative values indicate dispersed patterns or negative spatial autocorrelation, whereas positive values indicate clustered patterns or a positive spatial autocorrelation. Getis-Ord Gi* can generate a Z-score describing the degree of clustering of either high or low values, and has been widely used to detect hot and cold spots of disasters. The spatial pattern change analysis was conducted in ArcGIS 10.2.

3.3. Correlation Analysis

The linear regression model is widely used to evaluate the relationship between the two variables. Generally speaking, a set of observed data is known to be a dependent variable, and the other set is called the explanatory variable. The model is expressed as follows:

$$y = \alpha + \beta x, \tag{5}$$

where y is the dependent variable, x is the explanatory variable, α is the intercept, and β is the regression coefficient. The strength of the linear association between the two variables is commonly quantified by the

correlation coefficient, which is known as R^2. The value of R^2 is between 0 and 1, indicating the strength of the association of the observed data for the two variables. However, the R^2 value was affected by the number of explanatory variables. In this study, we use the adjusted R^2 to replace R^2, which eliminates the influence of the number of explanatory variables and can be calculated using Eq. (6).

$$R^2_{adjust} = 1 - \frac{n-1}{n-k-1}(1 - R^2), \tag{6}$$

where n is the number of observed data points and k is the number of explanatory variables.

3.4. Change-Point Analysis of Time Series

For the time series x1, x2,..., xn, s_k can be calculated using Eq. (7).

$$s_k = \sum_{i=1}^{k} r_i, \tag{7}$$

where

$$r_i = \begin{cases} 1, x_i > x_j \\ 0, x_i \le x_j \end{cases}, j = 1,2,\ldots,i; k = 1,2,\ldots,n. \tag{8}$$

Under the assumption of the independence of random samples in the time series,

$$UF_k = \frac{[s_k - E(s_k)]}{\sqrt{Var}(s_k)}, \tag{9}$$

where UF1 = 0 and E(Sk) and Var(Sk) are the mean and variance of the ordered column, respectively. For independent samples and the same continuous distribution, they can be calculated as follows:

$$E(s_k) = \frac{n(n+1)}{4}, \tag{10}$$

$$Var(s_k) = \frac{n(n-1)(2n+5)}{72}. \tag{11}$$

The value of UBk is calculated by reversing the time series and using the same method, where UBk = −UFk (k = n, n−1,...,1), and UB1 = 0. After analyzing and drawing the UBk and UFk curves, if the intersection of the two curves of UFk and UBk is between the critical lines, the value corresponding to the intersection is the time at which the mutation starts.

3.5. Prediction in Next Decade by Time Series

The ARIMA model is a common statistical model used for time-series forecasting. We hope to use the ARIMA model to predict future natural disasters. The ARIMA model has three parameters: p, d, and q. Parameter p is the number of lags in the time series data used in the prediction model, called the AR/autoregressive term; parameter d is the order of differentiation required to stabilize the time-series data, called the integrated term; and parameter q is the number of lags of the prediction error used in the prediction model, also called the MA/moving average term. ARIMA can be expressed as follows:

$$y(t) = \mu + \phi_1 * y(t-1) + \ldots + \phi_p * y(t-p) + \theta_1 * \varepsilon(t-1) + \ldots + \theta_q * \varepsilon(t-q), \tag{12}$$

where y is the difference sequence, ε is the noise sequence, φ is the coefficient of ARAR, and θ indicates the coefficient of MAMA.

4. Result

4.1. Temporal Pattern of Drought

As shown in Fig. (**1S**) (in Supplementary materials), drought within the four climatic zones showed different temporal patterns. The drought intensities of Henan Province and Inner Mongolia Province were higher than

those of Guizhou Province and Qinghai Province. At the time scales of 1-quarter- and 5- and 50-year intervals, the drought intensity of the four places all showed varying degrees of fluctuation over time. At the 1-quarter interval, although the amplitude of fluctuation in Guizhou Province is high, it is higher in Henan Province at 5- and 50-year intervals. The frequency of fluctuation in Henan Province and Inner Mongolia Province was higher at all time scales. In addition, we noticed that the temporal patterns of drought in Henan Province and Inner Mongolia Province were highly similar.

The M-K tests of droughts in the four provinces at time scales of 1-quarter and 1-, 5-, 10-, and 50-year intervals are shown in Table **1**. In Guizhou, Inner Mongolia, and Qinghai Provinces, at all intervals, the drought intensity showed an increasing trend. In Henan Province, the intensity shows an unexpected decreasing trend at 1-quarter and 1- and 5-year intervals, whereas at 10- and 50-year intervals, a non-significant increasing trend is shown. We also found that as the time scale increases, the Z value obtained by the M-K test decreases.

Table 1: M-K test of drought intensity at 1-quarter and 1-, 5-,10-, and 50-year intervals in four provinces.

Interval	Guizhou	Henan	Inner Mongolia	Qinghai
1-quarter	5.8887**	-2.5371	3.2346**	20.4200**
1-year	3.4800**	-1.5226	2.8231**	9.9245**
5-year	1.2187	-0.4497	1.6347	5.8681**
10-year	0.9318	0.0489	0.8190	5.1776**
50-year	1.1468	0.5213	0.7155	2.6833**

* Indicates the significance at 0.05 level; ** indicates the significance at 0.01 level

The analysis of change points in the time series is shown in Fig. (**S2**), where it can be seen that the change points of drought in each province are all after 1900. Between 1500 and 1650, the drought in Henan Province has several change points.

Based on the data collected and the results above, we attempted to establish the ARIMA model for the intensity of drought in the four provinces (Table **S1**). By substituting time t, the intensity of the natural disaster, y, at time t can be roughly predicted.

As shown in Fig. (**S3**), the drought intensities of the four seasons were extracted and analyzed separately, indicating varying temporal patterns. In Guizhou, Henan, and Qinghai Provinces, the difference in the intensity of drought in each season was not obvious. In Inner Mongolia Province, drought in winter and spring was stronger than that in summer and autumn.

The M-K test of drought in the four provinces in four separate seasons is shown in Table **2**. The seasonal difference in drought in Guizhou, Henan, and Qinghai Provinces is not obvious. Drought in Guizhou and Qinghai Provinces shows an increasing trend in the four seasons, and the drought in Henan Province shows a decreasing trend in the four seasons. In Inner Mongolia, there is an increasing trend of drought in spring and winter, but in summer and autumn, there is a non-significant increasing or decreasing trend in summer and autumn.

Table 2: M-K test of drought intensity of four seasons at the interval of 50 years.

Drought Time	Guizhou	Henan	Inner Mongolia	Qinghai
Spring	2.6656	-1.7551	3.8763	10.049
Summer	3.4801	-1.5087	0.6856	10.611
Autumn	2.6614	-1.0716	-0.081249	9.9575
Winter	2.9474	-0.78815	1.8561	10.253

4.2. Temporal Pattern of Flood

Similar to drought, floods also have varying temporal patterns in the four climatic zones (Fig. **S4**). The flood intensity of the four provinces is not much different, whereas the flood intensity in Henan Province is slightly higher than in the other three provinces. Before 1800, all four provinces showed slight fluctuations over time, among which Henan Province and Guizhou Province had a higher amplitude and frequency than the other two provinces. After 1800, the four provinces, particularly Inner Mongolia Province, showed an obvious increasing trend. The M-K test of floods in four provinces at time scales of 1-quarter and 1 -, 5-, 10-, and 50-year intervals are shown in Table **3**. The intensity of flood disasters in various provinces shows an increasing trend, particularly in the Inner Mongolia, Qinghai, and Guizhou Provinces. The flood intensity in Henan Province shows a slight increasing trend, and when the time scale is larger than the 5-year interval, the increasing trend is already non-significant.

Table 3: M-K test of flood intensity at 1-quarter and 1-, 5-, 10-, and 50-year intervals in four provinces.

Interval	Inner Mongolia	Qinghai	Henan	Guizhou
1-quarter	18.9910**	24.1130**	3.6463**	10.4180**
1-year	11.8570**	13.1720**	2.2877**	6.7368**
5-year	6.8080**	7.4303**	1.2479	4.2671**
10-year	5.2029**	5.6248**	0.8120	3.4456**
50-year	2.8622**	2.8143**	0.5213	1.9809*

The analysis of change points in the time series is shown in Fig. (**S5**), where it can be seen that the change points of floods in each province are all after 1900. Between 1500 and 1700, the flood in Henan Province has several change points. Based on the data collected and the results above, we attempted to establish the ARIMA model for the intensity of drought in the four provinces (Table **S2**). As shown in Fig. (**S6**), the flood intensities of the four seasons were extracted and analyzed separately, indicating varying temporal patterns. The summer flood is stronger, particularly in Henan Province. However, the Inner Mongolia flood also shows a higher intensity in spring, with an obvious increasing trend in recent years. The M-K test of droughts in the four provinces in four separate seasons is shown in Table **4**. There were no obvious seasonal differences in flooding. In only Henan Province, the increase in flooding in summer was slightly more significant than in other seasons.

Table 4: M-K test of flood intensity in four seasons at the interval of 50 years.

Flood Time	Guizhou	Henan	Inner Mongolia	Qinghai
Spring	5.619	1.7633	11.495	11.634
Summer	6.2826	3.1782	9.2901	13.367
Autumn	4.8365	1.5265	7.7988	12.093
Winter	4.1678	0.90051	9.3312	11.189

4.3. Temporal Pattern of Heavy Snow

As shown in Fig. (**S7**), the temporal snow patterns were diverse in the three climatic zones. Before 1800, the fluctuation frequency of snow disaster intensity was higher in Henan Province, and the amplitude was higher in Inner Mongolia Province. However, since 1800, the intensity of snow disasters in Qinghai Province has increased sharply, far surpassing Henan and Inner Mongolia Provinces, whereas the amplitude and frequency of its fluctuations are also extremely high. The M-K test of flooding in four provinces at time scales of 1-quarter, 1-, 5-, 10-, and 50-year intervals are shown in Table **5**. The intensity of snow disasters in all provinces showed an increasing trend. Among them, the increasing trend in Qinghai Province is more obvious, and the increasing trend of snow disaster intensity in Inner Mongolia and Henan Provinces is relatively slight.

Table 5: M-K test of snow intensity at 1-quarter and 1-, 5-, 10-, and 50-year intervals in three provinces.

Interval	Inner Mongolia	Qinghai	Henan
1-quarter	3.6640**	17.3250**	3.2793**
1-year	4.3872**	11.1780**	3.4978**
5-year	3.3096**	5.7745**	2.6361**
10-year	2.6151**	4.2540**	1.8911
50-year	0.7668	2.1359*	0.5213

The analysis of the change points in the time series is shown in Fig. (**S8**). Unlike droughts and floods, snow disasters have no obvious change points in Inner Mongolia and Qinghai Provinces. After 1900, only Henan Province had a change point. Based on the data collected and the results above, we attempted to establish the ARIMA model for the intensity of floods in the four provinces (Table **S3**). As shown in Fig. (**S9**), the snow intensities of the four seasons were separately extracted and analyzed, indicating varying temporal patterns. In Henan Province, snow disasters occur in spring, autumn, and winter, with a lower frequency in autumn. In recent years, snow disasters in winter have shown a decreasing trend, whereas it shows an increasing trend in spring. In Inner Mongolia Province, snow disasters occur mainly in winter. In Qinghai Province, snow disasters occur in all seasons, and there is an increasing trend after 1900. In the four seasons, the intensity of snow disasters in spring and winter was greater, and their increasing trend was more obvious.

The M-K test of snow in the four provinces in four separate seasons is shown in Table **6**. Similar to droughts, the seasonal difference in droughts in the Henan and Qinghai Provinces is not obvious. In Inner Mongolia, there is an increasing trend of drought in spring and winter, but in summer and autumn, there is a non-significant increasing or decreasing trend in summer and autumn.

Table 6: M-K test of snow intensity in four seasons at 50-year intervals.

Heavy Snow Time	Henan	Inner Mongolia	Qinghai
Spring	1.7305	2.4492	10.025
Summer	1.7908	-0.33786	7.3527
Autumn	2.1588	0.68374	8.3389
Winter	1.6975	3.158	8.7782

4.4. Spatial Pattern of Drought

Natural disasters in each province also exhibited an uneven spatial distribution pattern. According to Fig. (**S10**), the distribution of drought disasters in Guizhou Province is scattered. By contrast, the drought disasters in Henan Province show a pattern of distribution with more occurrences in the north and fewer in the south, although the distribution is still relatively scattered. The distribution of droughts in Inner Mongolia and Qinghai Provinces is concentrated. The drought in Inner Mongolia Province is concentrated in the south, and the drought in Qinghai Province is concentrated in the east. The Getis-Ord Gi* reflects the spatial pattern (Fig. **S11**). The hot spot of drought is distributed in the north of Guizhou and Henan Provinces, south of Inner Mongolia Province, and east of Qinghai Province. The cold spot is distributed in the south of Henan Province and southeast of Qinghai Province. According to Moran's I of the 100-year interval (Table **7**), for interannual instability, the spatial pattern of disasters also changes over time. The values of Moran's I varied from year to year, indicating that the spatial pattern was constantly changing. In Henan and Guizhou Provinces, most of the time, drought shows a nonsignificant cluster or dispersed patterns. It shows significant clustered patterns in Inner Mongolia Province. In Qinghai Province, there is a different pattern in different periods: a dispersed pattern during 1500-1599 and 1600-1699, a significant cluster pattern during 1700-1799, 1800-1899, and 1900-2000.

Table 7: Moran's I of drought in four provinces.

Period	Inner Mongolia	Qinghai	Henan	Guizhou
1500-1599	0.210851*	-0.068797	0.092226	0.013319
1600-1699	0.268892*	-0.078237*	0.171107*	0.052935
1700-1799	0.674934*	0.537597*	0.124287	-0.053365
1800-1899	0.845726*	0.4073*	-0.139473	0.042047
1900-1949	——	——	0.033549	0.142651*
-1987	0.438018*	——	——	——
-2000	——	0.37446*	——	——

The spatial distribution of the trend of the droughts in the four provinces is shown in Fig. (**1**). Most of the drought-affected counties in Guizhou Province showed an insignificant increasing or decreasing trend, which was scattered and staggered throughout the province. Few counties show a significant increasing and decreasing trend, and they are also scattered. In many countries in Henan Province, there are significant increasing and decreasing trends. The growth trend is concentrated in the west, and the decreasing trend is scattered in the east. At the same time, the insignificant increasing and decreasing trends were mostly distributed in the eastern region. In Inner Mongolia Province, drought shows a significant increasing trend in most areas, whereas it shows an insignificant increasing or decreasing trend in some areas of the northeast. In the south, drought shows a significant or insignificant decreasing trend. As for Qinghai Province, the drought shows significant increasing and decreasing trends in the northeast, and an insignificant decreasing trend in the northwest.

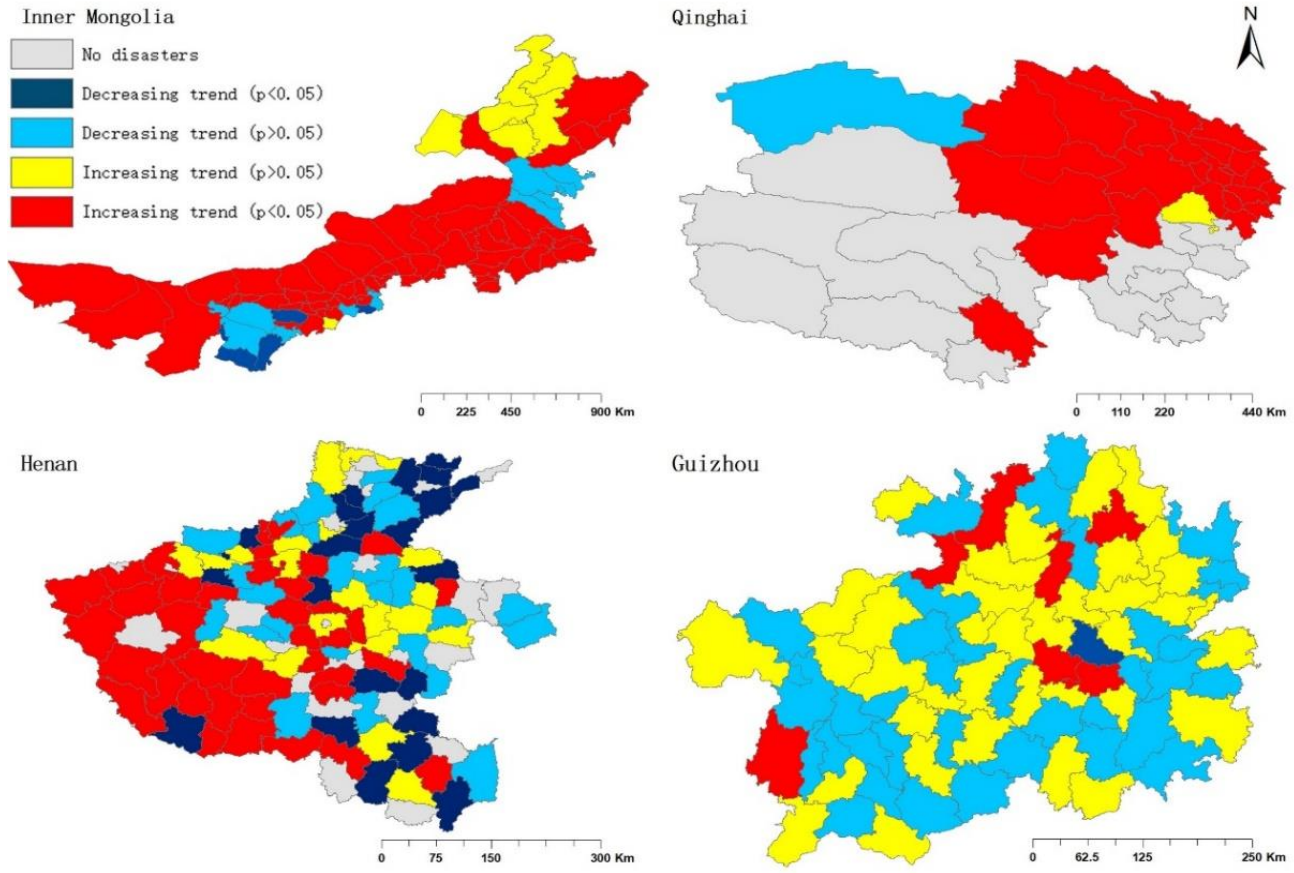

Figure 1: M–K tests of the change trends regarding drought intensity in the study areas.

As shown in Fig. (**S12**), the spatial distribution of drought in the four provinces has few seasonal differences and is similar to the overall distribution. According to Fig. (**S13**), in Guizhou Province, drought rarely shows a significant increasing or decreasing trend in the four seasons. It shows a non-significant increasing trend in most of the provinces in autumn and winter, whereas in spring and summer, it shows a non-significant decreasing trend in the east, west, and south regions. In the southwest of Inner Mongolia, drought in spring and winter showed a decreasing trend, whereas drought in summer and autumn showed an increasing trend. In Henan and Qinghai Provinces, there were no obvious seasonal differences in the spatial distribution of the drought trends.

4.5. Spatial Pattern of Flood

Similar to droughts, floods in Guizhou Province are scattered throughout the province (Fig. **S14**). They are also scattered in Henan Province, but there is an unobvious distribution pattern in which there are more in the east and fewer in the west. In Inner Mongolia, floods are mainly distributed in the south and southeast regions. In Qinghai Province, floods are concentrated in the east and west.

The results of the Getis-Ord Gi* are shown in Fig. (**S15**). In Guizhou and Henan provinces, there are no hot or cold spots. In Inner Mongolia Province, hot spots are distributed in the south and southeast, whereas cold spots are distributed in the north. In Qinghai Province, similar to drought, the hot spot is distributed in the east and the cold spot is distributed in the southeast. As shown in Table **8**, floods show dispersed patterns during each period in Henan and Guizhou, except in Guizhou during the periods of 1500-1599 and 1900-1949, which shows a cluster pattern. In Inner Mongolia, floods have clustered patterns. A nonsignificant dispersal pattern is shown during 1600-1699 and 1700-1799, and a significant cluster pattern is shown during the periods of 1800-1899 and 1900-2000 in Qinghai Province.

Table 8: Moran's I of flood in four provinces.

Period	Inner Mongolia	Qinghai	Henan	Guizhou
1500-1599	0.129453*	——	-0.04476	0.128892*
1600-1699	0.342736*	-0.068929	-0.055629	-0.04471
1700-1799	0.188906*	-0.022288	-0.010519	-0.028676
1800-1899	0.247935*	0.421006*	-0.0909	-0.084686
1900-1949	——	——	-0.118441	0.044183
-1987	0.410462*	——	——	——
-2000	——	0.447097*	——	——

The spatial distribution of flood trends in the four provinces is shown in Fig. (**2**). Floods have shown significant increasing trends in most counties of Guizhou, Inner Mongolia, and Qinghai Provinces. In Henan Province, floods show increasing trends in more areas and a decreasing trend in fewer areas. They were scattered throughout the province. In addition, in Henan and Inner Mongolia Provinces, floods tend to decrease in high-intensity areas, while in Guizhou and Qinghai Provinces, floods tend to increase in high-intensity areas. As shown in Fig. (**S16**), the spatial distribution of floods in the four provinces has few seasonal differences and is similar to the overall distribution.

According to Fig. (**S17**), the distribution of snow disasters in Henan Province is scattered. The snow disasters in Inner Mongolia Province are concentrated in the north, and in general, there is a pattern of distribution with more in the east and less in the west. Snow disasters in Qinghai Province are mainly concentrated in the southern part of the province, and there is generally a distribution pattern of more snow disasters in the east and fewer snow disasters in the west. The results of Getis-Ord Gi* are shown in Fig. (**S18**). Hot spots of snow appear in the north-central regions of Henan Province and Inner Mongolia Province, south of Qinghai Province. Cold spots of snow appear in the southwest of Inner Mongolia Province, and east and northeast of Qinghai Province.

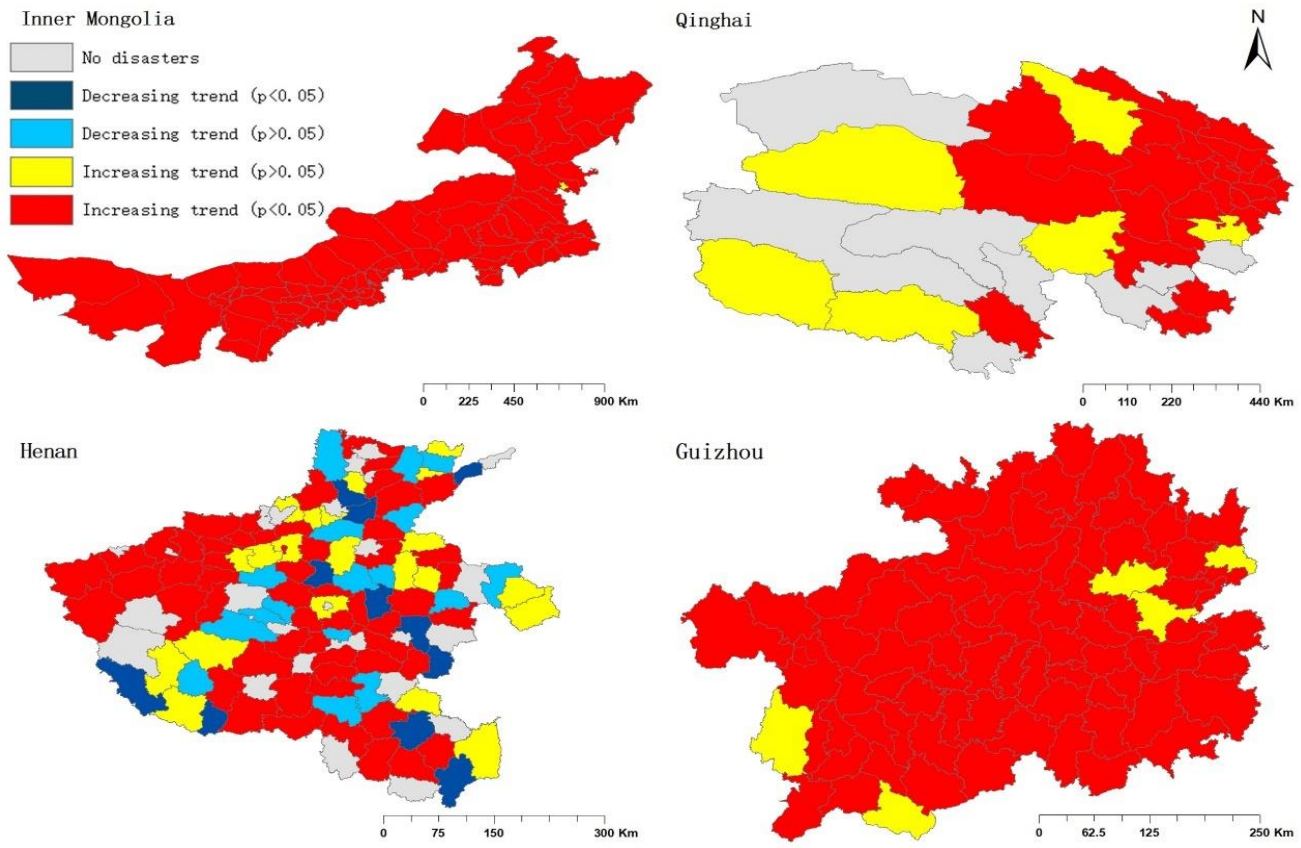

Figure 2: M–K tests of the change trends regarding flood intensity in the study areas.

As shown in Table **9**, snow in Henan shows a significant or nonsignificant cluster pattern. In Inner Mongolia, snow shows different patterns during different periods. A significant cluster pattern is shown during 1900–1949, a nonsignificant cluster pattern is shown during 1600-1699 and 1700-1799, and a random pattern is shown during 1800-1899. In Qinghai, a significant cluster pattern was shown during 1900–2000, whereas a dispersed pattern was shown at other times.

Table 9: Moran's I of snow in three provinces.

Period	Inner Mongolia	Qinghai	Henan
1500-1599	——	——	0.037559
1600-1699	0.105103*	-0.080493	0.189869*
1700-1799	0.112466*	——	0.056091
1800-1899	-0.005019	-0.008084	0.380919*
1900-1949	0.577575*	——	0.108535
-2000	——	0.30341*	——

The spatial distribution of snow trends in the four provinces is shown in Fig. (**3**). In Henan Province, counties with a significant increasing trend in snow disasters are relatively concentrated in the west, whereas counties with insignificant increasing or decreasing trends are scattered throughout the province. In the west of Inner Mongolia Province, snow disasters show a significant increasing trend, few of which show a significant increasing trend. In the east, snow disasters show an insignificant decreasing trend, and snow disasters in a few counties show an insignificant increasing trend. In all of Qinghai Province, there is a significant increasing trend of snow disasters. As shown in Fig. (**S19**), the spatial distribution of snow disasters in the four provinces has few seasonal differences and is similar to the overall distribution.

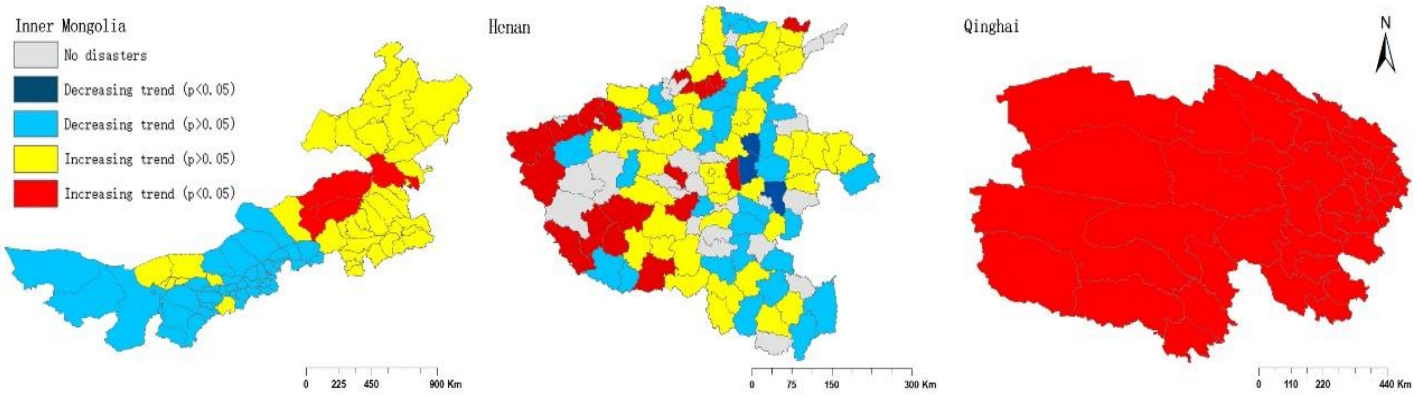

Figure 3: M–K tests of the change trends regarding snow intensity in the study areas.

According to Fig. (**S20**), in Inner Mongolia and Qinghai Provinces, the spatial distribution of disaster trends has few seasonal differences and is similar to the overall distribution. In Henan Province, the snow disasters in spring and summer show an increasing trend in the north and a decreasing trend in the south, whereas it is the opposite in autumn and winter.

5. Discussion

We took 500 years as the study period and 1-quarter and 1-, 5-, 10-, and 50-year periods as the temporal intervals to analyze the spatial and temporal patterns of the three main disasters in four climatic zones (subtropical, warm temperate, cold temperate, and plateau climate zones). We selected the Guizhou Province to represent China's subtropical regions, the Henan Province to represent the warm temperate regions, the Inner Mongolia Province to represent the cold temperate regions, and the Qinghai Province to represent plateau climate zones.

There were multiple temporal and spatial patterns associated with natural disasters in the different regions. There were also differences in the disaster intensities of the four provinces. The intensity of droughts in China's Henan and Inner Mongolia provinces was relatively high, whereas that in the Guizhou and Qinghai provinces was relatively low. China's drought intensity was higher in semiarid regions, similar to other regions in the world—such as the northeastern and southern parts of South America; the northern, southwestern, and Horn areas of Africa; Central Asia; Australia; the western US; and the Iberian Peninsula—and was lower in tropical regions, similar to the Amazon, Central Africa, and southern Asia [38-41]. There were few differences in the intensity of flooding in the four provinces, with a slightly higher intensity of flooding in the Henan Province. The intensity of snow disasters was much higher in the Qinghai Province than in other provinces, which may be due to its higher altitude. Through the MK test, we found that except for the slightly decreasing trend of droughts in the Henan Province, the three types of natural disasters showed an increasing trend in all four provinces in China. These results are similar to those previously reported [42, 43]. In addition, through a time-series analysis, we found that except for the snow disasters in the Inner Mongolia and Qinghai provinces, the change points of disasters in the four provinces all occurred after 1900.

The intensity of natural disasters in the Henan Province was relatively high, but its increasing trend was not obvious and there may even be a slightly decreasing trend. The disaster intensity fluctuated drastically over time, and the frequency and amplitude of the fluctuations were high. Natural disasters in the Inner Mongolia Province were extremely similar to those in the Henan Province. The intensity of natural disasters was slightly lower than that of the Henan Province, and the frequency and amplitude of intensity fluctuations over time were also slightly lower. However, the increasing trend of natural disasters in the Inner Mongolia Province was significant. Although the total intensity of natural disasters in the Guizhou Province was not higher than that in the Henan and Inner Mongolia provinces, fluctuations in the intensity of natural disasters over time were evident. This indicates that the regions in the Guizhou Province often experience severe disasters with a wide range of impacts and great losses. The Qinghai Province has unique climatic characteristics; therefore, natural disasters in that area are also unique.

Droughts and floods, which are more common in other regions, had lower intensities in the Qinghai Province. However, relatively rare snow disasters had an extremely high intensity in the Qinghai Province. The increasing trend in its natural disaster intensity was also far more pronounced, which may be caused by the greater impact of climate change [44].

The disasters were also analyzed separately for each season. The seasonal differences in the intensity of drought disasters in the Guizhou, Henan, and Qinghai provinces were not obvious, whereas those in the Inner Mongolia Province mostly occurred in winter and spring. In all four provinces, floods were concentrated in the summer. Snow disasters mainly occurred in winter and spring, but they still had high intensity in summer and autumn in the Qinghai Province. According to the MK test, the seasonal differences in disaster trends in the Guizhou, Henan, and Qinghai provinces were not obvious and were similar to the overall trend. However, the trends of disasters in the Inner Mongolia Province showed seasonal differences. Drought and snow disasters showed a significant increasing trend in winter and spring, but their trends were not significant in autumn and summer.

Overall, the spatial distribution of natural disasters in the Guizhou and Henan provinces was similar. The distribution of natural disasters and their changing trends were extremely scattered. In contrast, in the Inner Mongolia and Qinghai provinces, the distribution of natural disasters and the distribution of their changing trend always showed obvious clustering. In the Inner Mongolia Province, drought and floods were mainly concentrated in the south, (at low latitudes), whereas snow disasters were concentrated in the north (at high latitudes). In the Qinghai Province, the distributions of droughts and floods were extremely similar, concentrated in the east, while snow disasters were distributed in the south, which is an area with high altitudes and extensive snowcapped mountains. Ballesteros–Cánovas *et al*. (2015) pointed out that climate warming enhances the snow avalanche risk in the Western Himalayas [45]. This is similar to the spatial pattern indicated by Moran's I. In cold temperate areas and the Qinghai province, the disasters showed a cluster distribution, whereas in the Guizhou and Henan provinces, they often showed a non-significant cluster or even a dispersed distribution.

In general, the spatial distribution of disaster intensity had few seasonal differences and was similar to the overall distribution. However, when we analyzed the spatial distribution of disaster trends by season separately, we found that drought in most of the Guizhou Province showed a non-significant increasing trend in autumn and winter and a non-significant decreasing trend in eastern, western, and southern Guizhou in the spring and summer. There were no clear seasonal differences in the spatial distribution of the flood trends. In the Henan Province, there were no evident seasonal differences in the spatial distribution of the drought trends. More central counties showed a significantly increasing trend of flooding in the summer, while the opposite was observed in the winter. Snow disasters in spring and summer showed an increasing trend in the north and a decreasing trend in the south, whereas the opposite was true in autumn and winter. In the Inner Mongolia Province, drought in the southwest showed a decreasing trend in spring and winter and an increasing trend in summer and autumn. There was no clear seasonal difference in the spatial distribution of flooding and snow disaster trends. The differences in natural disasters in the eastern and western areas of Inner Mongolia may have been caused by climatic differences. Western Inner Mongolia is controlled by a continental climate, whereas Eastern Inner Mongolia has an Asian monsoon climate and is strongly affected by East Asian monsoons [10]. In the plateau climate zone, perhaps owing to the small seasonal changes in temperature and precipitation, the spatial distribution of the disaster trends had no clear seasonal difference, which is similar to the overall distribution [46].

Owing to the influence of topography, latitude, altitude, population, and human activities, differences in the spatial and temporal patterns of natural disasters in different regions within the same climatic zone were observed, despite the provinces that best represent the climatic zones being chosen. The possible loss in the records may have led to relatively fewer data in earlier years. The study of natural disasters, particularly the temporal-spatial pattern, could support the mitigation of natural disasters and improve the management practices of environmental systems in a large-scale region []. For a deeper understanding of the temporal and spatial patterns of natural disasters in various climate zones, more research is needed in the future, particularly concerning the interval of climate change, spatial movement trends of disasters, and mutual influence between disasters.

6. Conclusion

China has experienced increasingly frequent natural disasters, including droughts, floods, and heavy snowfall from 1500 to 2000. During the 500 years, the intensity of drought in Henan and Inner Mongolia was higher than that in Guizhou and Qinghai, while little difference in flood intensity was observed among these provinces. The intensity of snow disasters in Qinghai was much higher. Except for the slightly decreasing drought trend in Henan, the three natural disasters showed a significant increase over time. Drought disasters in Guizhou, Henan, and Qinghai showed few seasonal differences, whereas those in Inner Mongolia mostly occurred in winter and spring. Floods were concentrated during the summer, while snow disasters occurred mainly during winter and spring. According to the MK test, the seasonal differences in disaster trends in Guizhou, Henan, and Qinghai were unclear and similar to the overall trend. The spatial distribution of natural disasters in Guizhou and Henan were similar, and their changing trends were extremely scattered, while in Inner Mongolia and Qinghai, they were clustered. The spatial distribution of disaster intensity had few seasonal differences and was similar to the overall distribution. Seasonal variation, spatial movement, force drivers, and mutual influence of natural hazards during the 500 years need to be further studied, to detailly derive their occurrence interval and rhythm and determine the corresponding prevention and combating.

Authors Contributions

YP designed the study and revised the paper. ZW and JY carried out the calculations and wrote the paper. YP, ZW, JY, CW, and GL collected the data and supported it with their experience and literature studies.

Conflict of Interest

The Authors declare no conflict of interest.

Data Availability

The data that support the findings of this study are available from the corresponding author upon reasonable request.

Acknowledgments

We want to express our appreciation to editors and reviewers for their valuable suggestions. The research was funded by the Top Discipline and First-class University Constriction Project (ydzxxk202018) of Minzu University of China.

Supplementary Material

The supplementary material is available below the article.

References

[1] Easterling DR, Meehl GA, Parmesan C, Changnon SA, Karl TR, Mearns LO. Climate extremes: observations, modeling, and impacts. Science (1979) 2000; 289: 2068-74. https://doi.org/10.1126/science.289.5487.2068

[2] Xu W, Ma L, Ma M, Zhang H, Yuan W. Spatial–temporal variability of snow cover and depth in the qinghai–tibetan plateau. J Climate. 2017; 30: 1521–33. https://doi.org/10.1175/JCLI-D-15-0732.1

[3] Du X, Jin X, Yang X, Yang X, Xiang X, Zhou Y. Spatial-temporal pattern changes of main agriculture natural disasters in China during 1990–2011. J Geogr Sci. 2015; 25: 387-98. https://doi.org/10.1007/s11442-015-1175-x

[4] McMichael AJ, Woodruff RE, Hales S. Climate change and human health: present and future risks. The Lancet. 2006; 367: 859-69. https://doi.org/10.1016/S0140-6736(06)68079-3

[5] Morrissey SA, Reser JP. Natural disasters, climate change and mental health considerations for rural Australia. Aust J Rural Health. 2007; 15: 120-5. https://doi.org/10.1111/j.1440-1584.2007.00865.x

[6] Fengjin X, Ziniu X. Characteristics of tropical cyclones in China and their impacts analysis. Natural Hazards. 2010; 54: 827–37. https://doi.org/10.1007/s11069-010-9508-7

[7] Kim S, Shin Y, Kim H, Pak H, Ha J. Impacts of typhoon and heavy rain disasters on mortality and infectious diarrhea hospitalization in South Korea. Int J Environ Health Res. 2013; 23: 365-76. https://doi.org/10.1080/09603123.2012.733940

[8] Ni J, Sun L, Li T, Huang Z, Borthwick AGL. Assessment of flooding impacts in terms of sustainability in mainland China. J Environ Manage. 2010; 91: 1930-42. https://doi.org/10.1016/j.jenvman.2010.02.010

[9] Liu J, Diamond J. China's environment in a globalizing world. Nature. 2005; 435: 1179-86. https://doi.org/10.1038/4351179a

[10] Huang J, Xue Y, Sun S, Zhang J. Spatial and temporal variability of drought during 1960–2012 in Inner Mongolia, north China. Quat Int. 2015; 355: 134-44. https://doi.org/10.1016/j.quaint.2014.10.036

[11] Wang A, Lettenmaier DP, Sheffield J. Soil Moisture Drought in China, 1950–2006. J Clim. 2011; 24: 3257-71. https://doi.org/10.1175/2011JCLI3733.1

[12] Su B, Kundzewicz ZW, Jiang T. Simulation of extreme precipitation over the Yangtze River Basin using Wakeby distribution. Theor Appl Climatol. 2009; 96: 209-19. https://doi.org/10.1007/s00704-008-0025-5

[13] Zhai J, Su B, Krysanova V, Vetter T, Gao C, Jiang T. Spatial variation and trends in PDSI and SPI indices and their relation to streamflow in 10 large regions of China. J Climate. 2010; 23: 649-63. https://doi.org/10.1175/2009JCLI2968.1

[14] FAO. Report of FAO-CRIDA Expert Group Consultation on Farming System and Best Practices for Drought-Prone Areas of Asia and the Pacific Region. Food and Agricultural Organization of United Nations; Central Research Institute for Dryland Agriculture: Hyderabad, India, 2002.

[15] Von Buttlar J, Zscheischler J, Rammig A, Sippel S, Mahecha MD. Impacts of droughts and extreme-temperature events on gross primary production and ecosystem respiration: A systematic assessment across ecosystems and climate zones. Biogeosciences. 2018; 15: 1293–1318. https://doi.org/10.5194/bg-15-1293-2018

[16] World Bank. India, Financing Rapid Onset Natura Disaster Losses in India: A Risk Management Approach. Washington, DC: 2003.

[17] Li M, Li S, Li Y. Studies on drought in the past 50 years in China. Chin J Agrometeorol. 2003; 24: 8-11.

[18] Li Y, Ye W, Wang M, Yan X. Climate change and drought: a risk assessment of crop-yield impacts. Clim Res. 2009; 39: 31-46. https://doi.org/10.3354/cr00797

[19] Liu Z. Comprehensive analysis of drought disasters in China. Disaster Adv. 2012: 1275–80.

[20] Qiu H, Cao M, Hao J, Wang Y, Wang Y. Relationship between frequency and magnitude of drought damage in China. Sci Geogr Sin. 2013; 33: 576–80.

[21] Long D, Shen Y, Sun A, Hong Y, Longuevergne L, Yang Y, *et al*. Drought and flood monitoring for a large karst plateau in Southwest China using extended GRACE data. Remote Sens Environ. 2014; 155: 145–60. https://doi.org/10.1016/j.rse.2014.08.006

[22] Jongman B, Hochrainer-Stigler S, Feyen L, Aerts JCJH, Mechler R, Botzen WJW, *et al*. Increasing stress on disaster-risk finance due to large floods. Nat Clim Chang. 2014; 4: 264–8. https://doi.org/10.1038/nclimate2124

[23] Forzieri G, Feyen L, Russo S, Vousdoukas M, Alfieri L, Outten S, *et al*. Multi-hazard assessment in Europe under climate change. Clim Change. 2016; 137: 105–19. https://doi.org/10.1007/s10584-016-1661-x

[24] Paprotny D, Morales-Nápoles O. Estimating extreme river discharges in Europe through a Bayesian network. Hydrol Earth Syst Sci. 2017; 21: 2615–36. https://doi.org/10.5194/hess-21-2615-2017

[25] Vousdoukas MI, Mentaschi L, Voukouvalas E, Verlaan M, Feyen L. Extreme sea levels on the rise along Europe's coasts. Earths Future. 2017; 5: 304–23. https://doi.org/10.1002/2016EF000505

[26] Smith A, Bates PD, Wing O, Sampson C, Quinn N, Neal J. New estimates of flood exposure in developing countries using high-resolution population data. Nat Commun. 2019; 10: Article number: 1814. https://doi.org/10.1038/s41467-019-09282-y

[27] Wang R, Jiang T, Gao J, Chen J. Yangtze River flood: Causes and analysis. J Nat Disasters. 1999; 8: 16-20.

[28] Huicong J, Donghua P. On the spatial and temporal patterns of flood and drought hazards of China. Disaster Adva. 2013; 6: 12–8.

[29] Koenig U, Abegg B. Impacts of climate change on winter tourism in the swiss alps. J Sustain Tour. 1997; 5: 46-58. https://doi.org/10.1080/09669589708667275

[30] Keller F, Goyette S, Beniston M. Sensitivity analysis of snow cover to climate change scenarios and their impact on plant habitats in alpine terrain. Clim Change. 2005; 72: 299-319. https://doi.org/10.1007/s10584-005-5360-2

[31] Geis J, Strobel K, Liel A. Snow-induced building failures. J Perform Constr Fac. 2012;26:377–88. https://doi.org/10.1061/(ASCE)CF.1943-5509.0000222

[32] Taylor DA. A survey of snow loads on the roofs of arena-type buildings in Canada. Can J Civil Eng. 1979; 6: 85–96. https://doi.org/10.1139/l79-010

[33] Zhang J. Risk assessment of drought disaster in the maize-growing region of Songliao Plain, China. Agr Ecosyst Environ. 2004; 102: 133–53. https://doi.org/10.1016/j.agee.2003.08.003

[34] Qin Z, Tang H, Li W, Zhang H, Zhao S, Wang Q. Modelling impact of agro-drought on grain production in China. Int J Disast Risk Reduct. 2014; 7: 109-21. https://doi.org/10.1016/j.ijdrr.2013.09.002

[35] Zhou Y, Li N, Wu W, Wu J, Gu X, Ji Z. Exploring the characteristics of major natural disasters in China and their impacts during the past decades. Nat Hazards. 2013; 69: 829-43. https://doi.org/10.1007/s11069-013-0738-3

[36] Peng Y, Long S, Ma J, Song J, Liu Z. Temporal-spatial variability in correlations of drought and flood during recent 500 years in Inner Mongolia, China. Science of The Total Environment. 2018; 633: 484-91. https://doi.org/10.1016/j.scitotenv.2018.03.200

[37] Peng Y, Song J, Cui T, Cheng X. Temporal–spatial variability of atmospheric and hydrological natural disasters during recent 500 years in Inner Mongolia, China. Natural Hazards. 2017; 89: 441–56. https://doi.org/10.1007/s11069-017-2973-5

[38] Seager R, Ting M, Held I, Kushnir Y, Velez J. Model projections of an imminent transition to a more arid climate in southwestern North America. Science (1979). 2007; 316: 1181–4. https://doi.org/10.1126/science.1139601

[39] Dai A. Drought under global warming: a review. WIREs Climate Change. 2011; 2: 45-65. https://doi.org/10.1002/wcc.81

[40] Spinoni J, Naumann G, Carrao H, Barbosa P, Vogt J. World drought frequency, duration, and severity for 1951-2010. Int J Climatol. 2014; 34: 2792-804. https://doi.org/10.1002/joc.3875

[41] Güneralp B, Güneralp İ, Liu Y. Changing global patterns of urban exposure to flood and drought hazards. Global Environ Chang. 2015; 31: 217-25. https://doi.org/10.1016/j.gloenvcha.2015.01.002

[42] Xu J, Shi Y, Gao X, Giorgi F. Projected changes in climate extremes over China in the 21st century from a high resolution regional climate model (RegCM3). Chinese Sci Bull. 2013; 58: 1443–52. https://doi.org/10.1007/s11434-012-5548-6

[43] Ji Z, Kang S. Evaluation of extreme climate events using a regional climate model for China. Int J Climatol. 2015; 35: 888-902. https://doi.org/10.1002/joc.4024

[44] Alfieri L, Burek P, Feyen L, Forzieri G. Global warming increases the frequency of river floods in Europe. Hydrol Earth Syst Sci. 2015; 19: 2247–60. https://doi.org/10.5194/hess-19-2247-2015

[45] Ballesteros-Cánovas JA, Trappmann D, Madrigal-González J, Eckert N, Stoffel M. Climate warming enhances snow avalanche risk in the Western Himalayas. Proc Natl Acad Sci USA. 2018; 115: 3410–5. https://doi.org/10.1073/pnas.1716913115

[46] Bernard E, Naveau P, Vrac M, Mestre O. Clustering of maxima: Spatial dependencies among heavy rainfall in France. J Clim. 2013; 26: 7929–37. https://doi.org/10.1175/JCLI-D-12-00836.1

Supplementary Materials

Table S1: ARIMA of drought intensity in four provinces.

Province	Interval	ARIMA Formula
Guizhou	1-quarter	y(t)=2.543+0.073*y(t-1)+0.711*ε(t-1)+0.624*ε(t-2)+0.504*ε(t-3)
	1-year	y(t)=-0.0-0.475*y(t-1)
Henan	1-quarter	y(t)=8.144+0.05*y(t-1)+0.823*y(t-2)-0.107*y(t-3)-0.1*y(t-4) +0.066*y(t-5)+0.007*y(t-6)-0.024*y(t-7)-0.017*y(t-8)+0.946*ε(t-1)
	1-year	y(t)=32.716+0.52*y(t-1)-0.07*y(t-2)
Inner Mongolia	1-quarter	y(t)=0.012-0.999*y(t-1)+0.421*ε(t-1)-0.927*ε(t-2)-0.379*ε(t-3)
	1-year	y(t)=0.368-0.364*y(t-1)
Qinghai	1-quarter	y(t)=0.002+0.162*y(t-1)+0.013*y(t-2)-0.341*y(t-3)+0.224*y(t-4) -0.383*ε(t-1)-0.156*ε(t-2)+0.273*ε(t-3)-0.693*(t-4)
	1-year	y(t)=0.031-0.496*y(t-1)

Table S2: ARIMA of flood intensity in four provinces.

Province	Interval	ARIMA Formula
Guizhou	1-quarter	y(t)=0.003+0.513*y(t-1)+0.087*y(t-2)
	1-year	y(t)=10.062+0.969*y(t-1)-0.919*ε(t-1)
Henan	1-quarter	y(t)=5.707-0.174*y(t-1)+0.656*y(t-2)-0.169*y(t-3)+0.994*ε(t-1)
	1-year	y(t)=22.662+0.875*y(t-1)-0.776*ε(t-1)
Inner Mongolia	1-quarter	2.678+0.822*y(t-1)-0.3*ε(t-1)
	1-year	y(t)=12.0+0.797*y(t-1)-0.681*ε(t-1)+0.306*ε(t-2)
Qinghai	1-quarter	y(t)=1.205-0.27*y(t-1)+0.574*y(t-2)-0.013*y(t-3) +0.129*y(t-4)-0.011*y(t-5)+0.955*ε(t-1)
	1-year	y(t)=0.06-0.79*y(t-1)-0.171*ε(t-1)-0.592*ε(t-2)

Table S3: ARIMA of flood intensity in four provinces.

Province	Interval	ARIMA Formula
Guizhou	1-quarter	y(t)=2.071+0.876*y(t-1)-0.051*y(t-2)-0.108*y(t-3)-0.353*ε(t-1)
	1-year	y(t)=10.062+0.969*y(t-1)-0.919*ε(t-1)
Henan	1-quarter	y(t)=5.711+0.645*y(t-1)-0.999*y(t-2)+0.645*y(t-3)+0.16*ε(t-1) +1.081*ε(t-2)+0.032*ε(t-3)
	1-year	y(t)=22.662+0.875*y(t-1)-0.776*ε(t-1)
Inner Mongolia	1-quarter	y(t)=0.0-0.983*y(t-1)-0.004*ε(t-1)-0.981*ε(t-2)-0.015*ε(t-3)
	1-year	y(t)=12.0+0.797*y(t-1)-0.681*ε(t-1)+0.306*ε(t-2)
Qinghai	1-quarter	y(t)=1.205-0.27*y(t-1)+0.574*y(t-2)-0.013*y(t-3)+0.129*y(t-4) -0.011*y(t-5)+0.955*ε(t-1)
	1-year	y(t)=0.06-0.79*y(t-1)-0.171*ε(t-1)-0.592*ε(t-2)

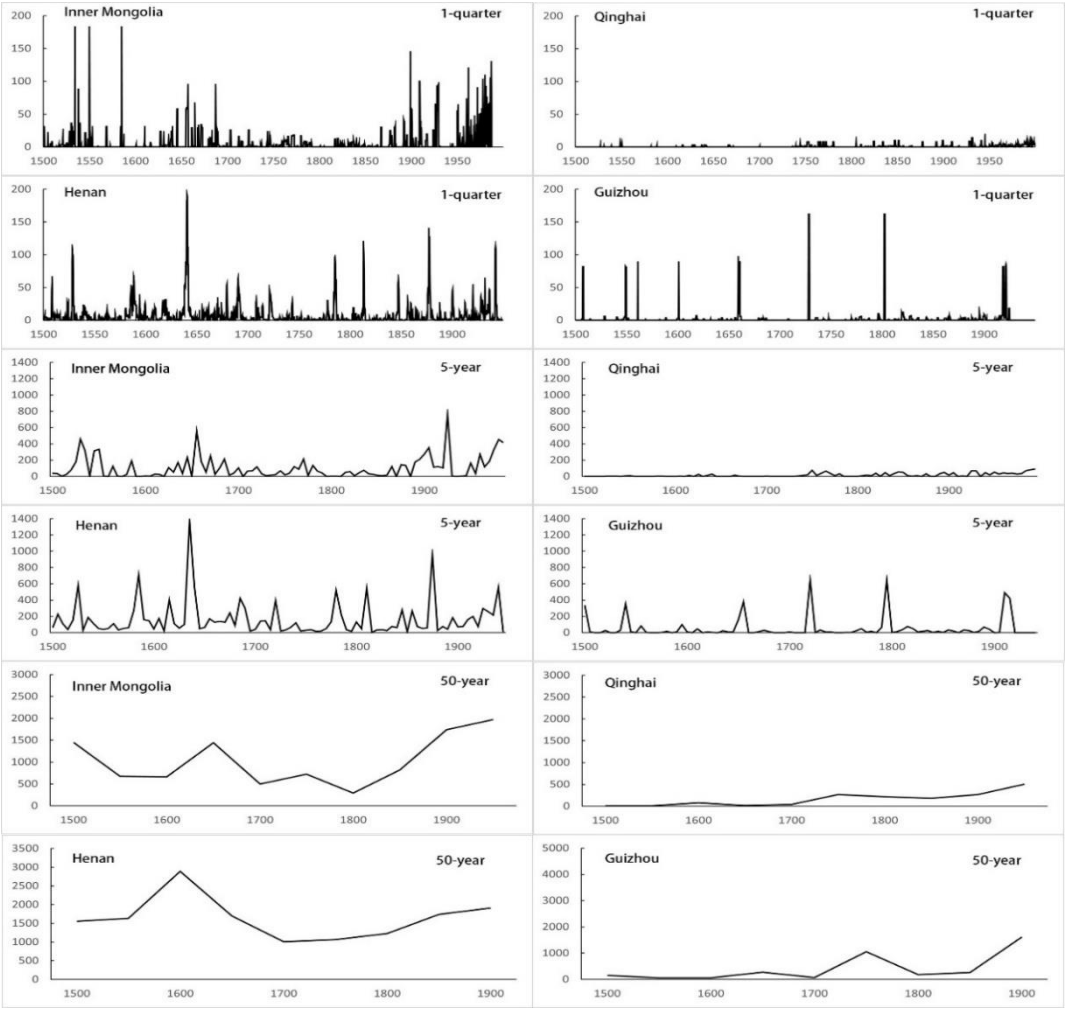

Figure S1: Intensity of drought at time scales of 1-quarter and 5- and 50-year intervals in four provinces.

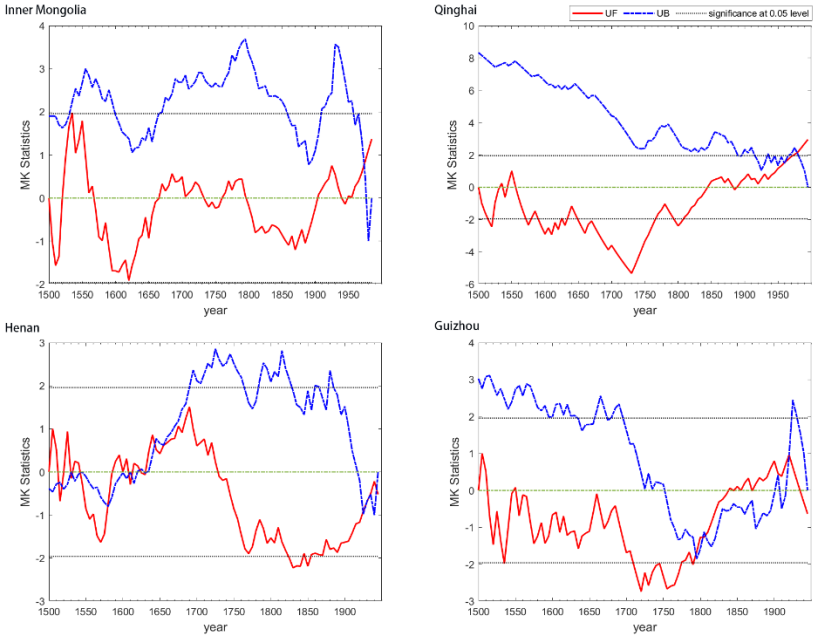

Figure S2: Change-point analysis of drought in four provinces.

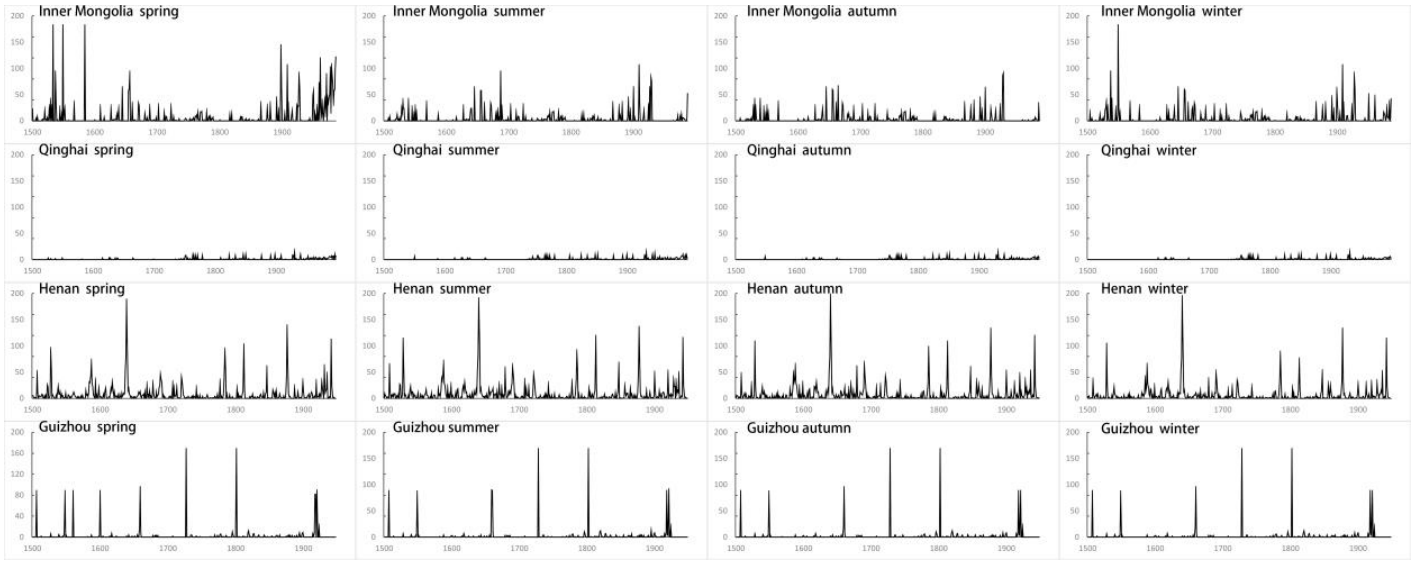

Figure S3: Drought intensity of four seasons in four provinces.

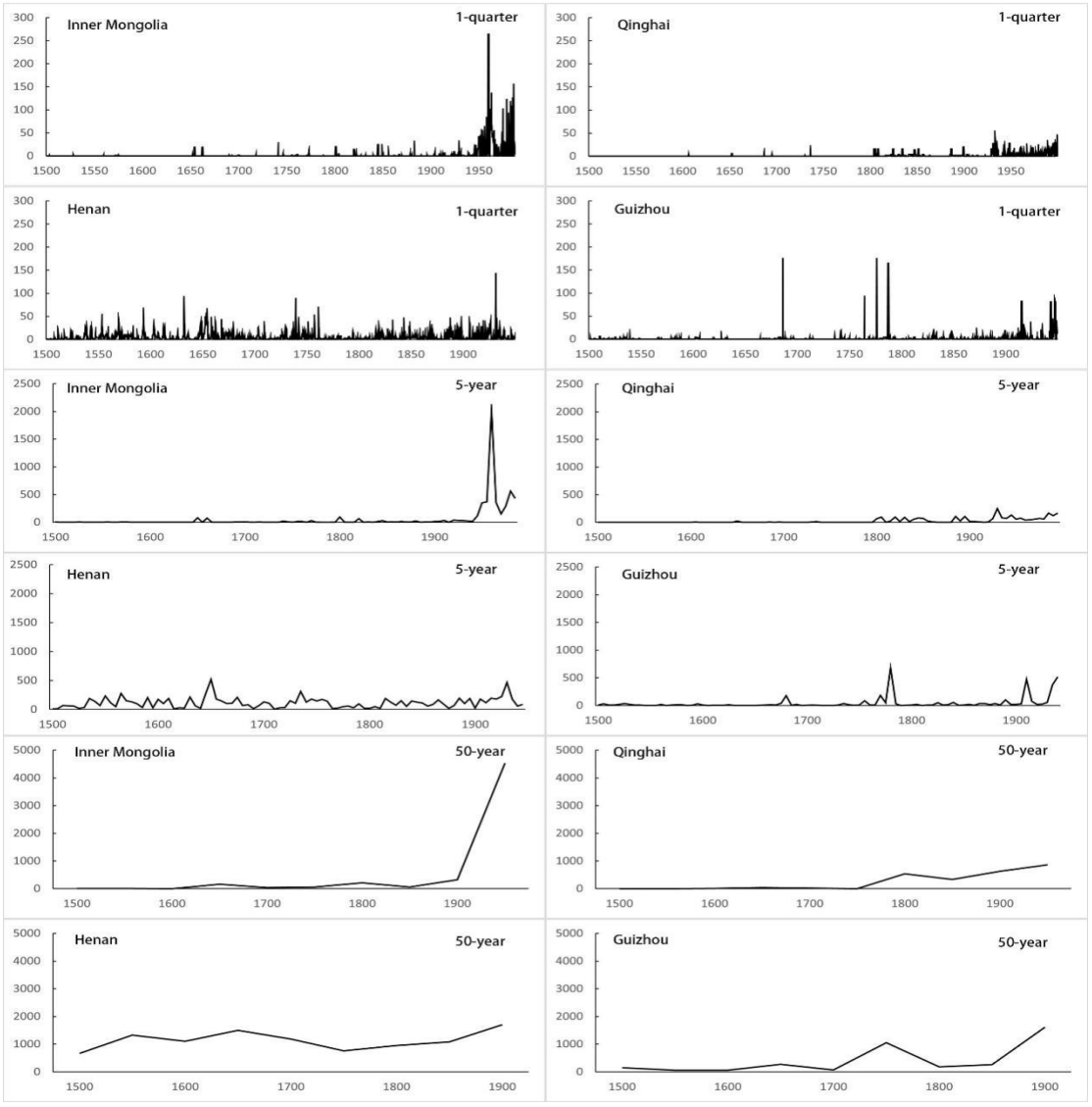

Figure S4: Intensity of floods at the time scales of 1-quarter and 5- and 50-year intervals in four provinces.

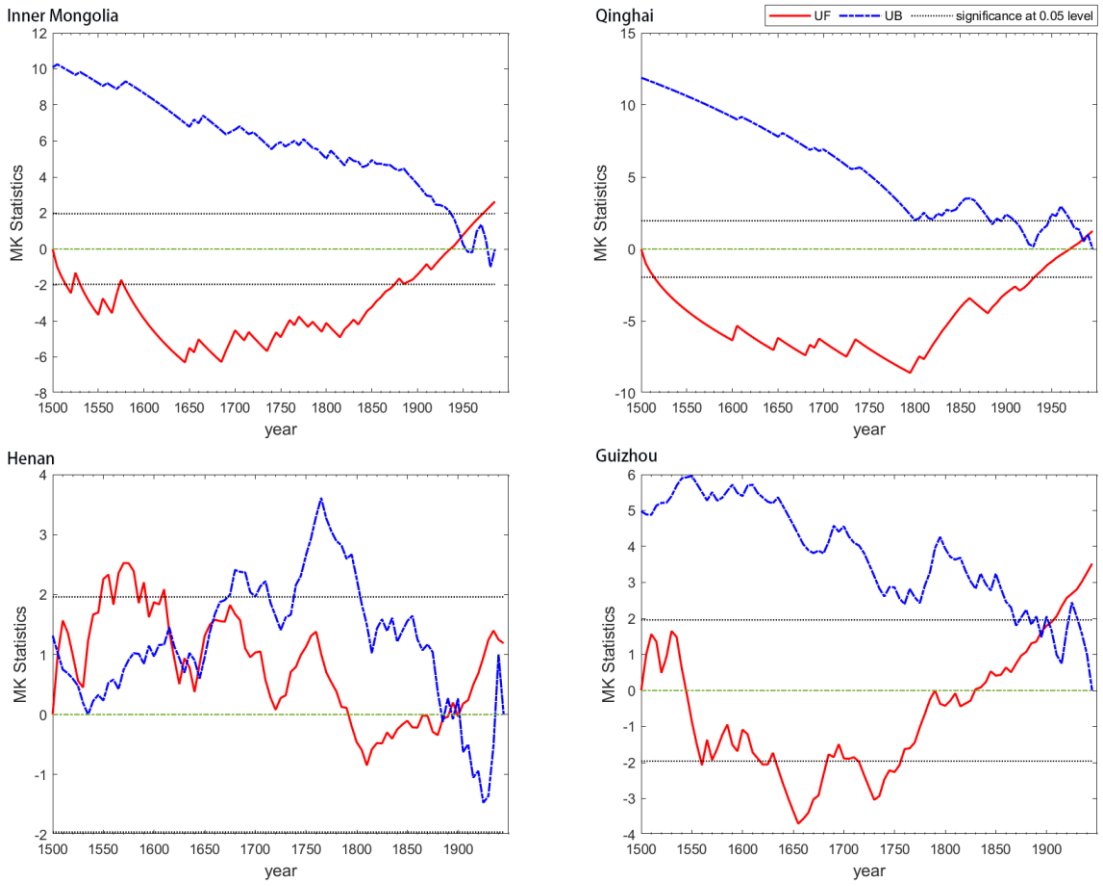

Figure S5: Change-point analysis of flood in four provinces.

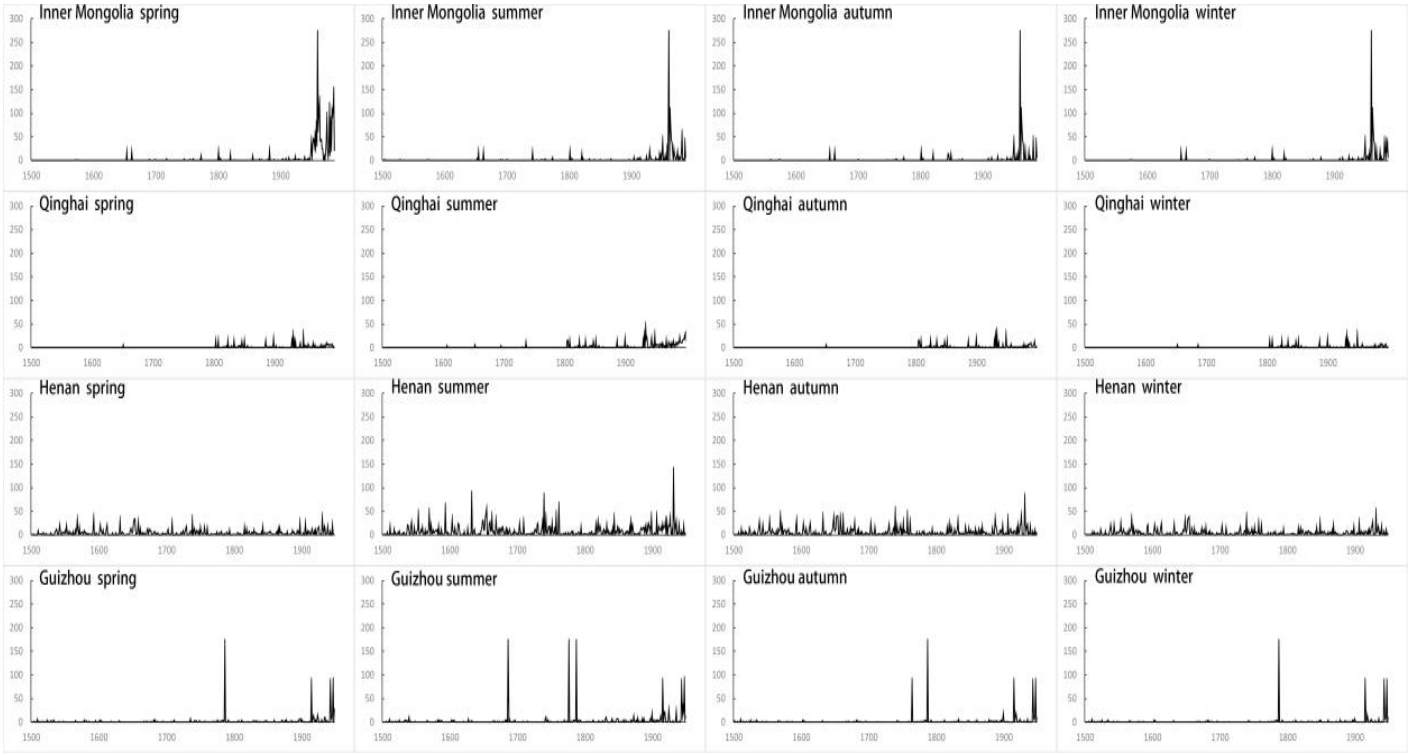

Figure S6: Flood intensity of four seasons in four provinces.

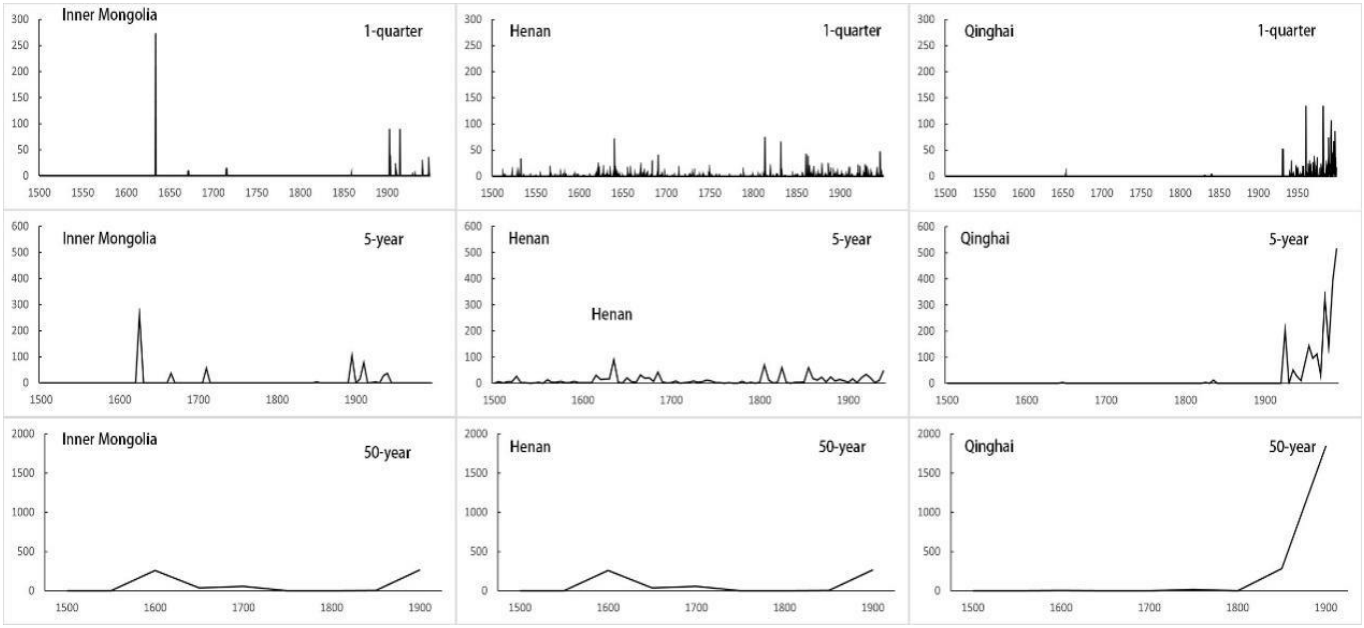

Figure S7: Intensity of snow at the time scale of 1-quarter and 5- and 50-year intervals in four provinces.

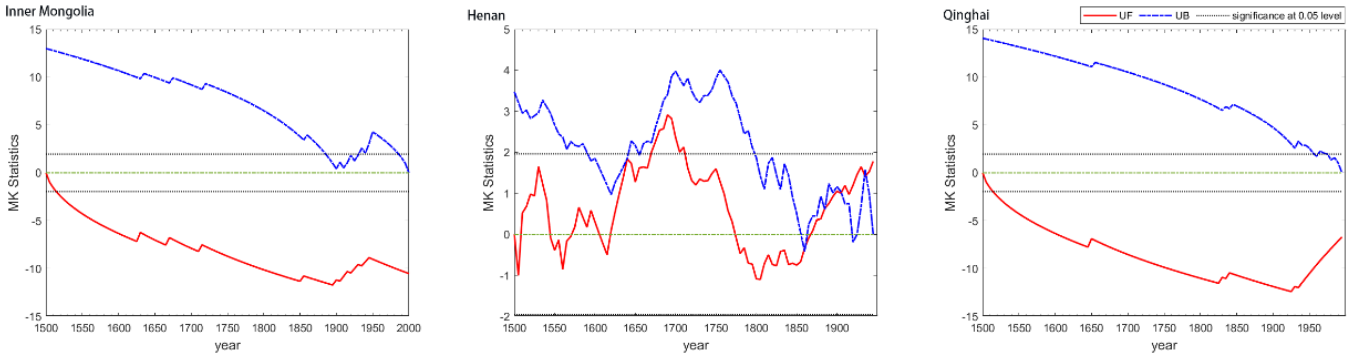

Figure S8: Change-point analysis of drought in four provinces.

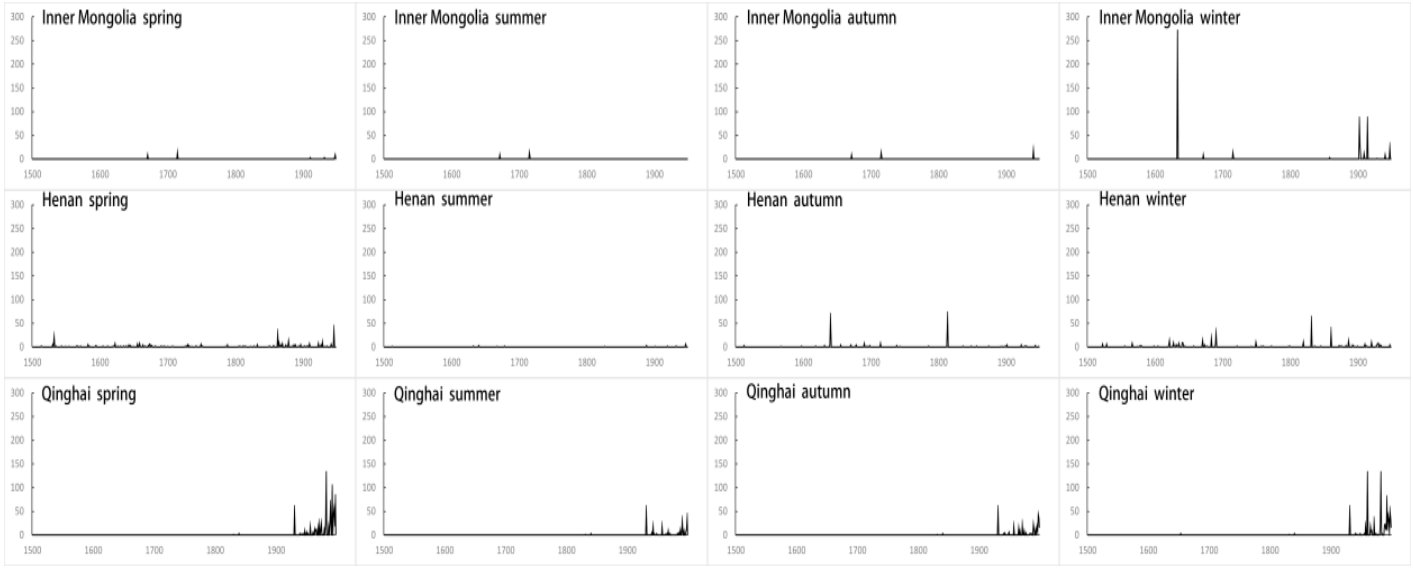

Figure S9: Snow intensity of four seasons in four provinces.

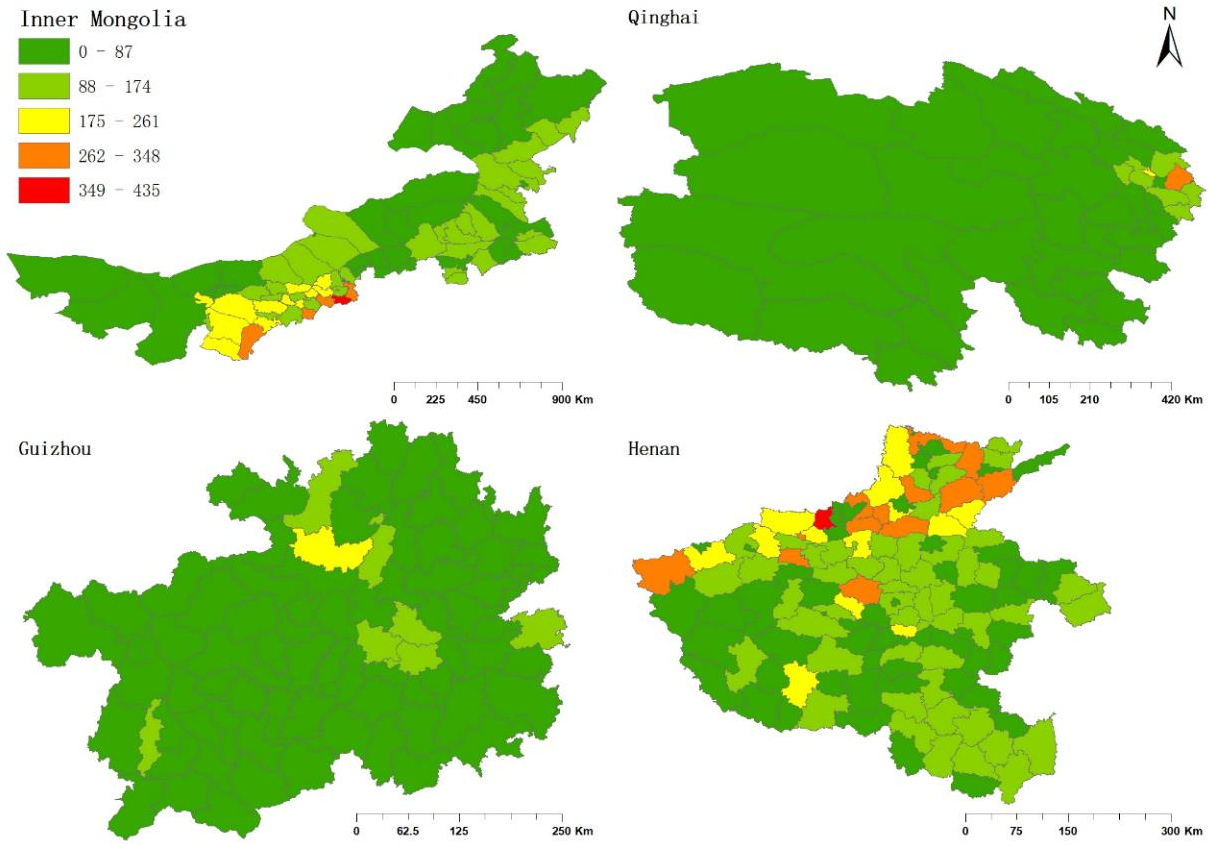

Figure S10: Overall spatial distribution of drought in four provinces.

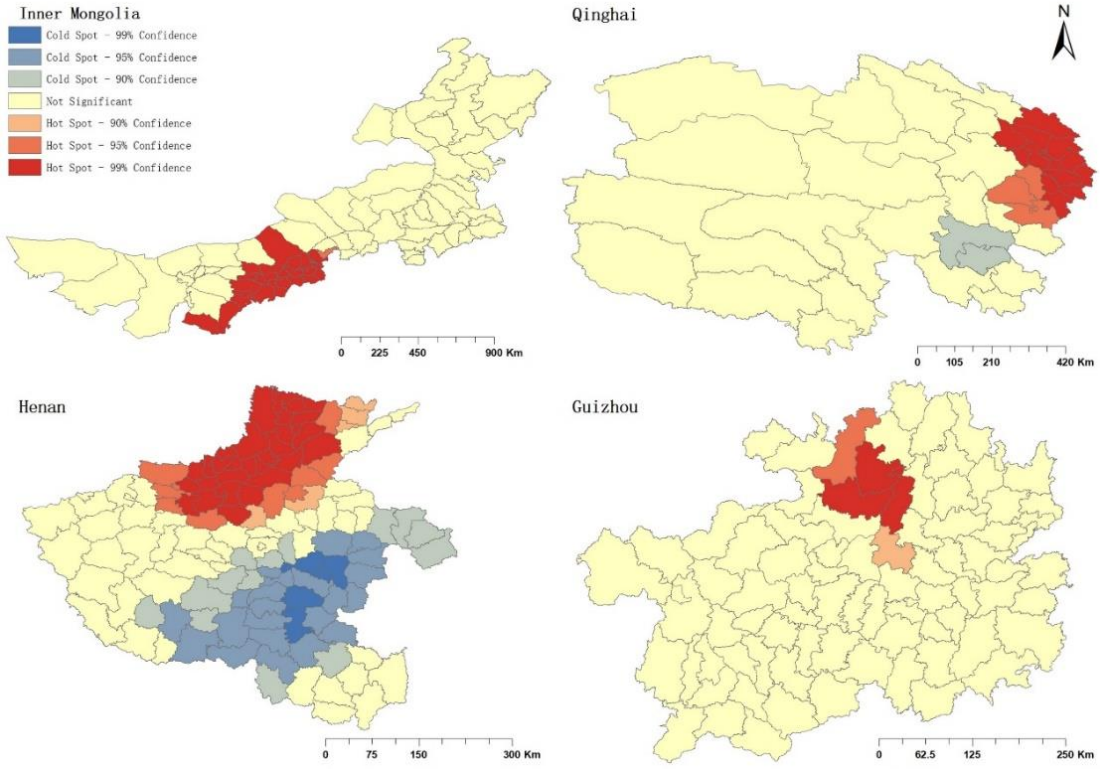

Figure S11: Getis-Ord Gi* of drought intensity in four provinces.

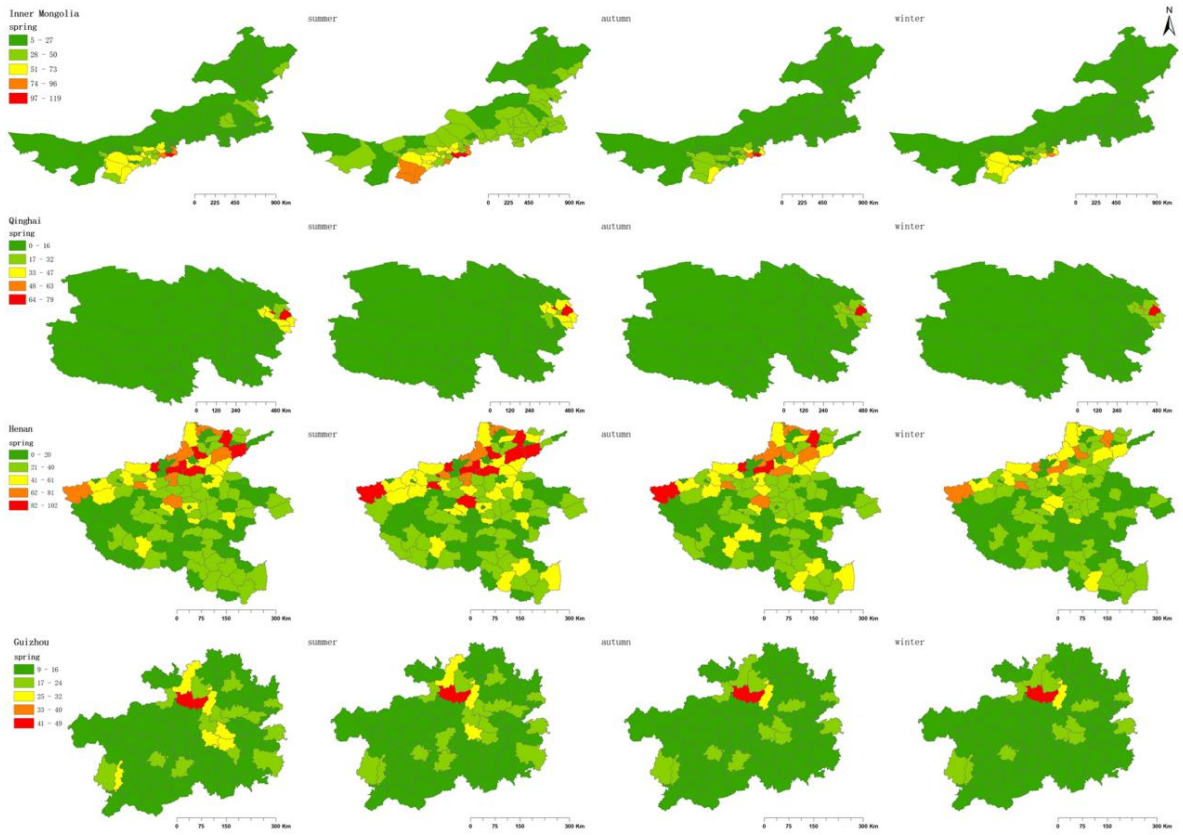

Figure S12: Spatial distribution of drought in four seasons.

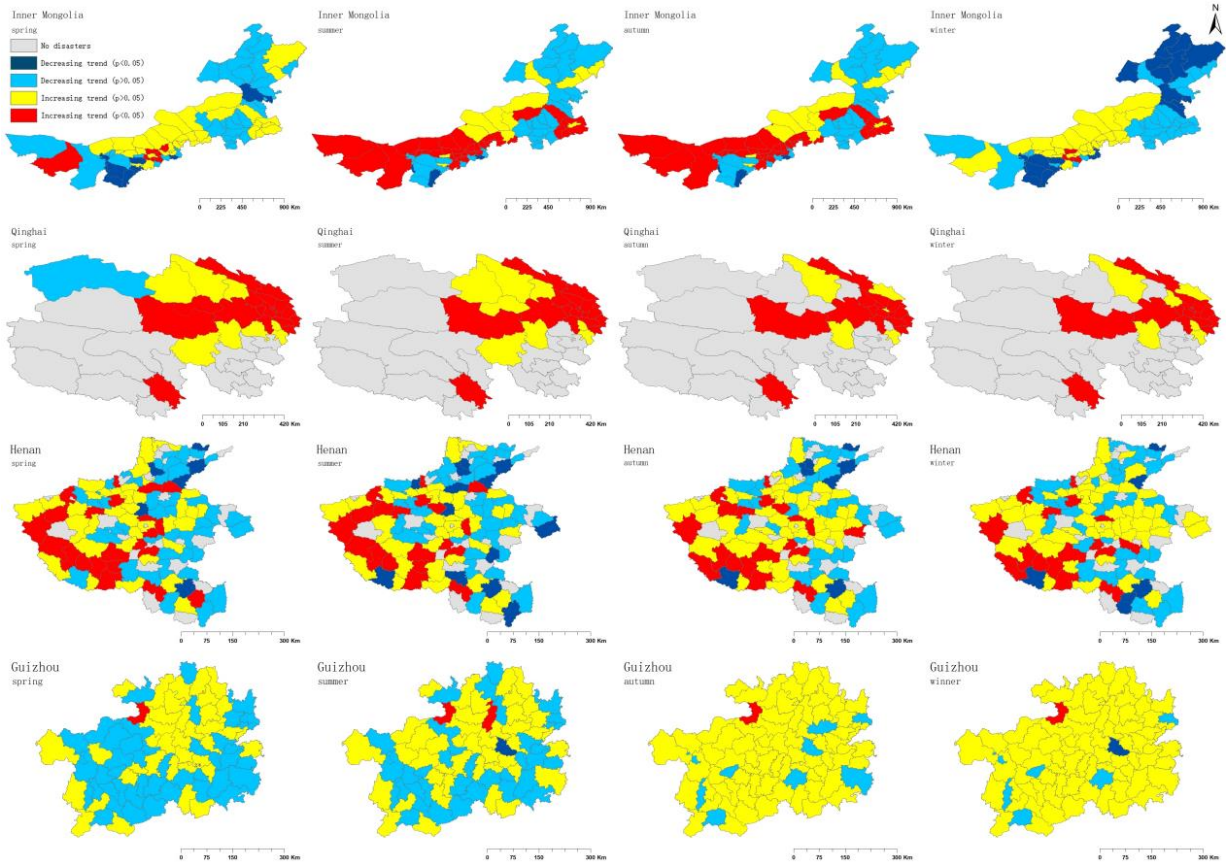

Figure S13: Spatial distribution of drought trends in four seasons.

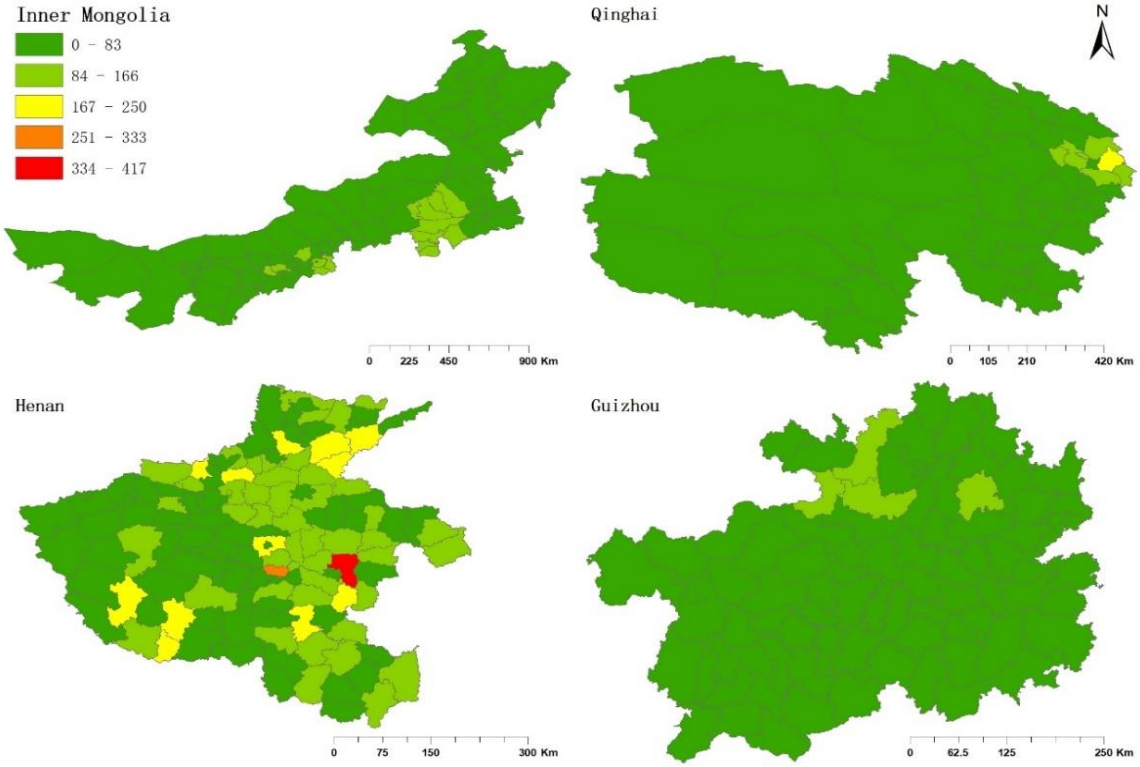

Figure S14: Overall spatial distribution of flood in four provinces.

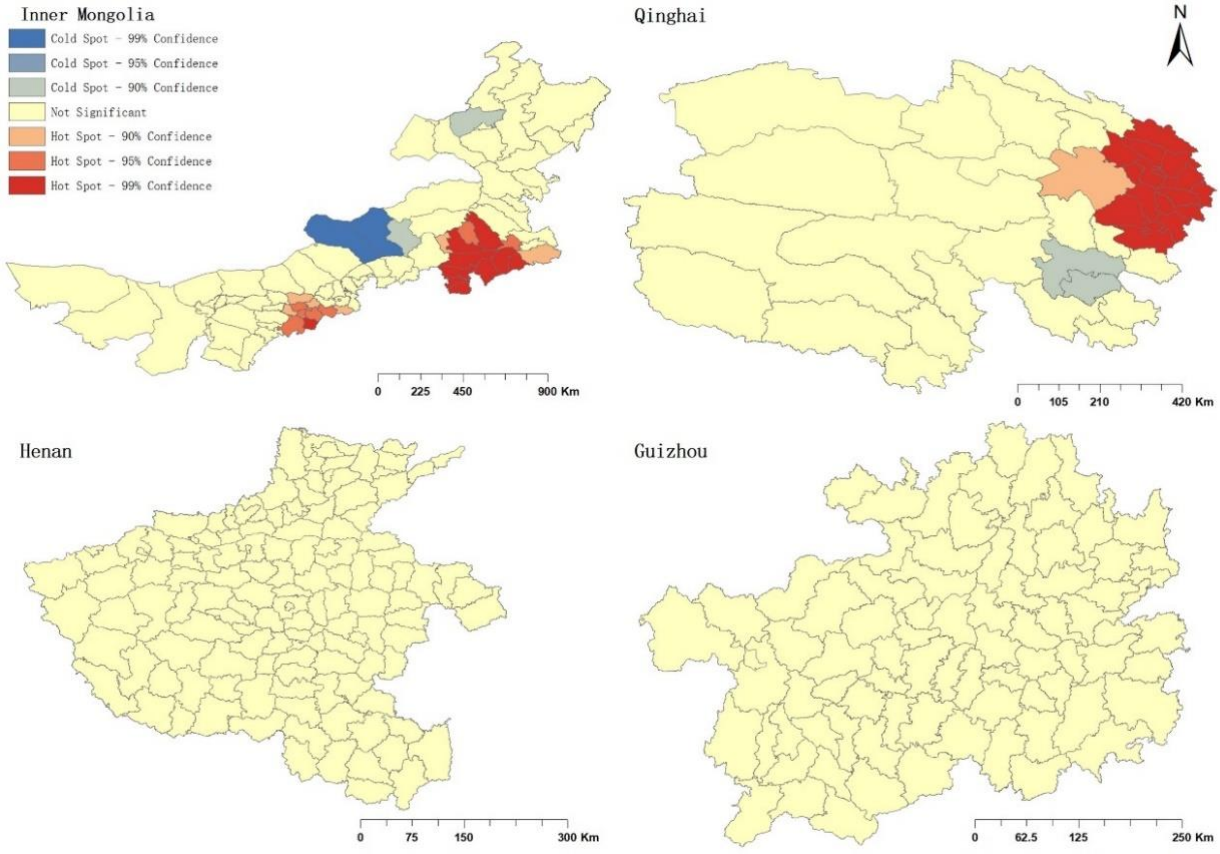

Figure S15: Getis-Ord Gi* of flood intensity in four provinces.

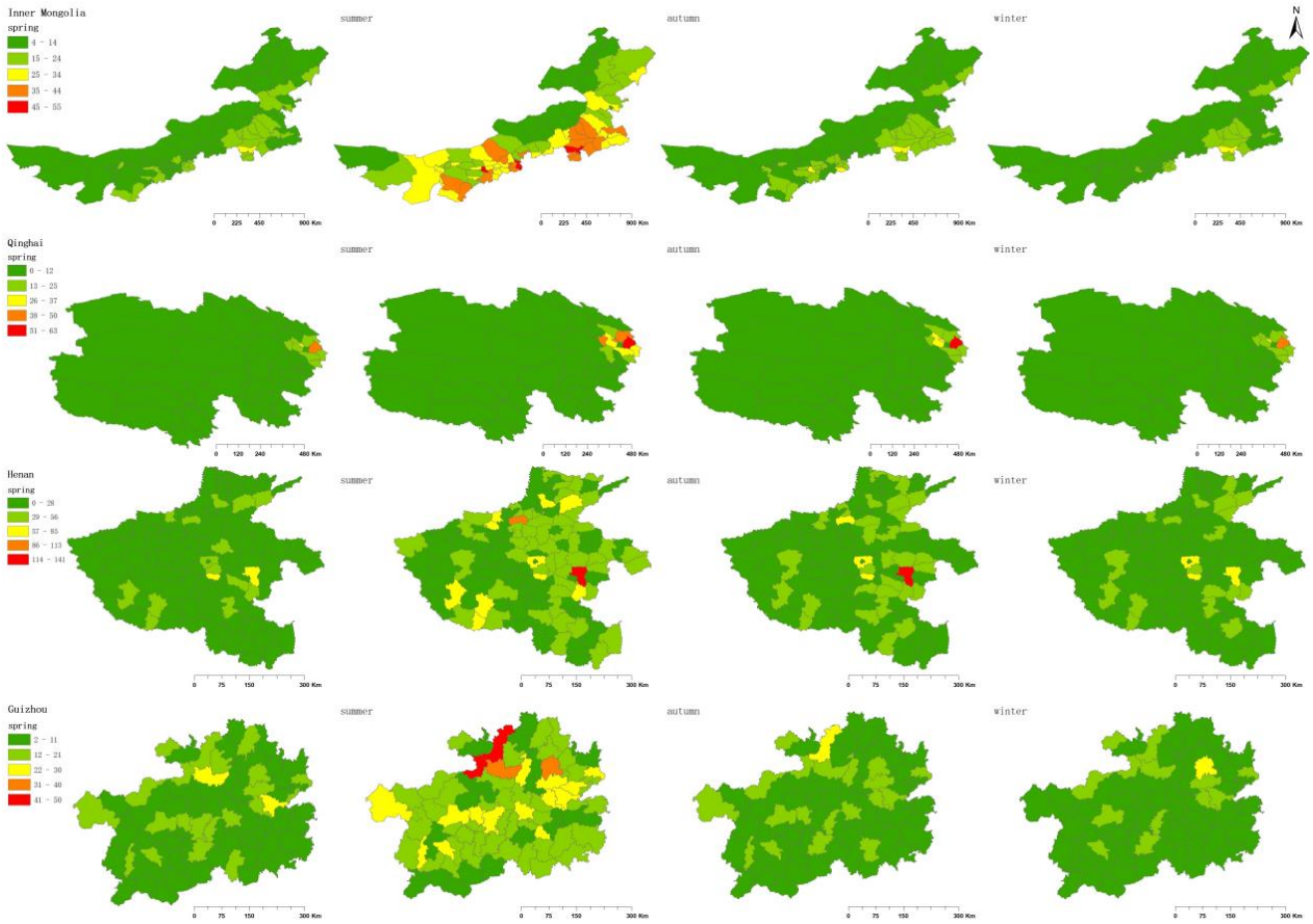

Figure S16: Spatial distribution of floods in four seasons.

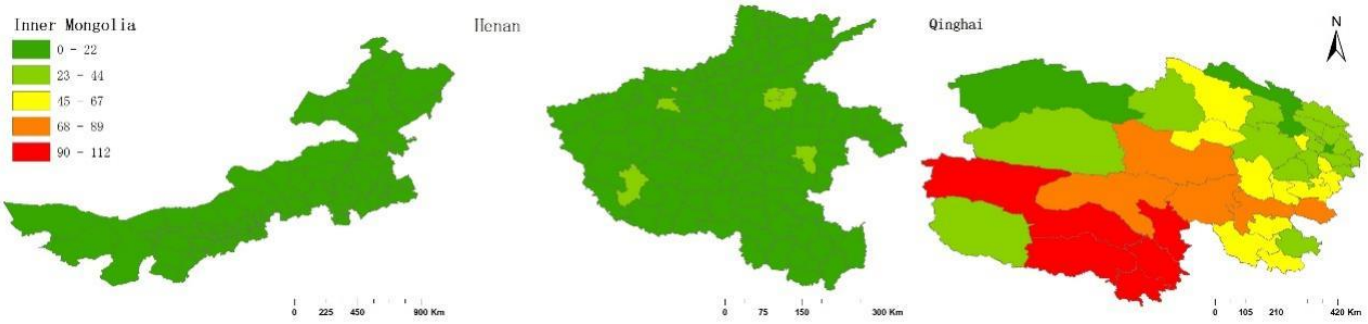

Figure S17: Overall spatial distribution of snow in four provinces.

Figure S18: Getis-Ord Gi* of snow disaster intensity in three provinces.

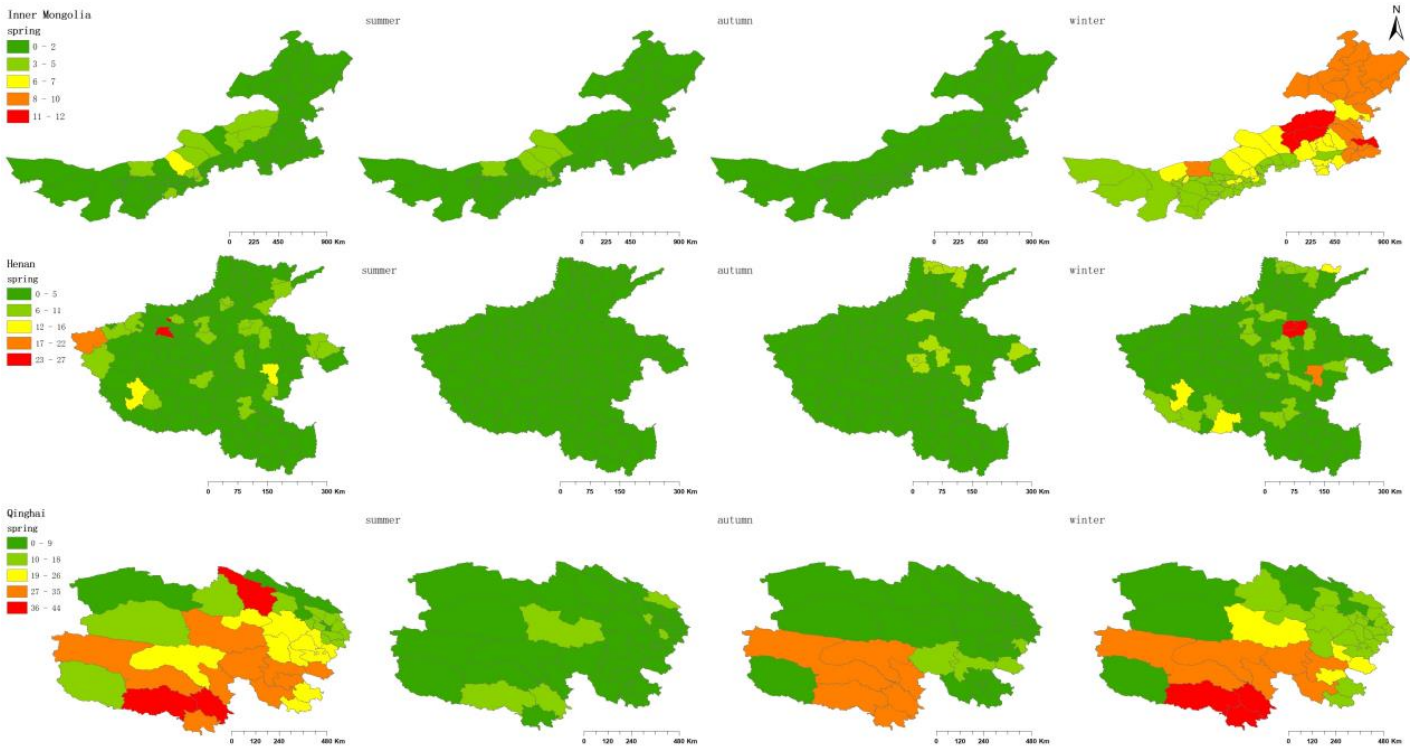

Figure S19: Spatial distribution of snow in four seasons.

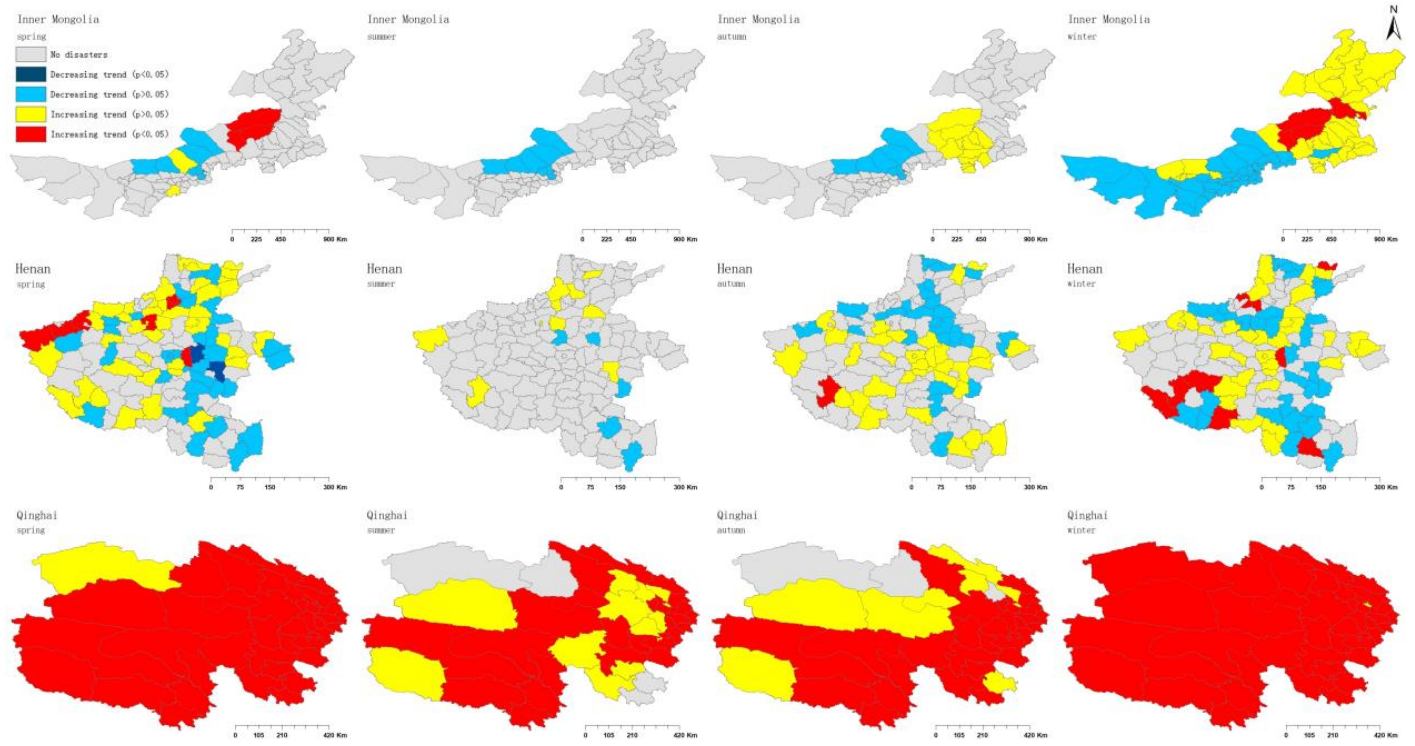

Figure S20: Spatial distribution of snow trends in four seasons.